

Institute of Geophysical Researches
National Nuclear Center
Kazakhstan Republic

**SEISMIC RECORDING CHARACTERIZATION
OF THE MAKANCHI OBSERVATORY**

(report on the contract F61708-96-W0317)

DISTRIBUTION STATEMENT A
Approved for public release
Distribution Unlimited

DTIC QUARTER 1998

19980423 033

Almaty, 1998

REPORT DOCUMENTATION PAGE

Form Approved OMB No. 0704-0188

Public reporting burden for this collection of information is estimated to average 1 hour per response, including the time for reviewing instructions, searching existing data sources, gathering and maintaining the data needed, and completing and reviewing the collection of information. Send comments regarding this burden estimate or any other aspect of this collection of information, including suggestions for reducing this burden to Washington Headquarters Services, Directorate for Information Operations and Reports, 1215 Jefferson Davis Highway, Suite 1204, Arlington, VA 22202-4302, and to the Office of Management and Budget, Paperwork Reduction Project (0704-0188), Washington, DC 20503.

1. AGENCY USE ONLY (Leave blank)		2. REPORT DATE 1998	3. REPORT TYPE AND DATES COVERED Final Report	
4. TITLE AND SUBTITLE Seismic Recording Characterization of the Makanchi Observatory			5. FUNDING NUMBERS F6170896W0317	
6. AUTHOR(S) Dr. Igor Komarov				
7. PERFORMING ORGANIZATION NAME(S) AND ADDRESS(ES) Institute of Geophysical Research 490 021 Semipalatinsk-21 Kazakhstan Republic Russia			8. PERFORMING ORGANIZATION REPORT NUMBER N/A	
9. SPONSORING/MONITORING AGENCY NAME(S) AND ADDRESS(ES) EOARD PSC 802 BOX 14 FPO 09499-0200			10. SPONSORING/MONITORING AGENCY REPORT NUMBER SPC 96-4092	
11. SUPPLEMENTARY NOTES Report includes informational report "Investigations on the Planned Seismic Array."				
12a. DISTRIBUTION/AVAILABILITY STATEMENT Approved for public release; distribution is unlimited.			12b. DISTRIBUTION CODE A	
13. ABSTRACT (Maximum 200 words) This report results from a contract tasking Institute of Geophysical Research as follows: The contractor shall perform three primary tasks as described in the proposal. The contractor shall characterize seismic noise and measure the power spectral densities of the ambient ground noise at Makanchi. All measurements will be compared to the Peterson "Low noise Model". 2) Characterize seismic signals and analyze seismograms from large (mb>=5) earthquakes and explosions and characterize the recording site.				
14. SUBJECT TERMS Geophysics			15. NUMBER OF PAGES 58	
			16. PRICE CODE N/A	
17. SECURITY CLASSIFICATION OF REPORT UNCLASSIFIED	18. SECURITY CLASSIFICATION OF THIS PAGE UNCLASSIFIED	19. SECURITY CLASSIFICATION OF ABSTRACT UNCLASSIFIED	20. LIMITATION OF ABSTRACT UL	

CONTENT

INTRODUCTION.....	3
1. GEOGRAPHICAL LOCATION OF MAKANCHI SEISMOLOGICAL STATION.....	4
2. GEOLOGICAL AND TECTONIC DESCRIPTION OF THE AREA OF THE MAKANCHI SEISMIC STATION.	6
3. A DESCRIPTION OF SEISMOLOGICAL EQUIPMENT, INSTALLED ON THE STATION.	12
4. DATA SELECTION AND DATA PROCESSING.....	14
5.THE ANALYSIS OF BACKGROUND SEISMIC NOISE.	17
6.THE RECORDS OF UNDERGROUND NUCLEAR EXPLOSIONS AND EARTHQUAKES.	30
CONCLUSION	39
REFERENCES.....	39

Introduction.

The geophysical observatory 'Makanchi' is one of the number of seismological observatories of the Institute of Geophysical Researches of National Nuclear Center of Kazakhstan Republic (IGR NNC RK) (Figure 1), destined for the monitoring of nuclear explosions, in compliance with 'Comprehensive Nuclear Test Ban Treaty'. The main purpose of Makanchi observatory is recording, detection and discrimination of underground nuclear explosions, since seismological methods are the most effective methods to decide this task.

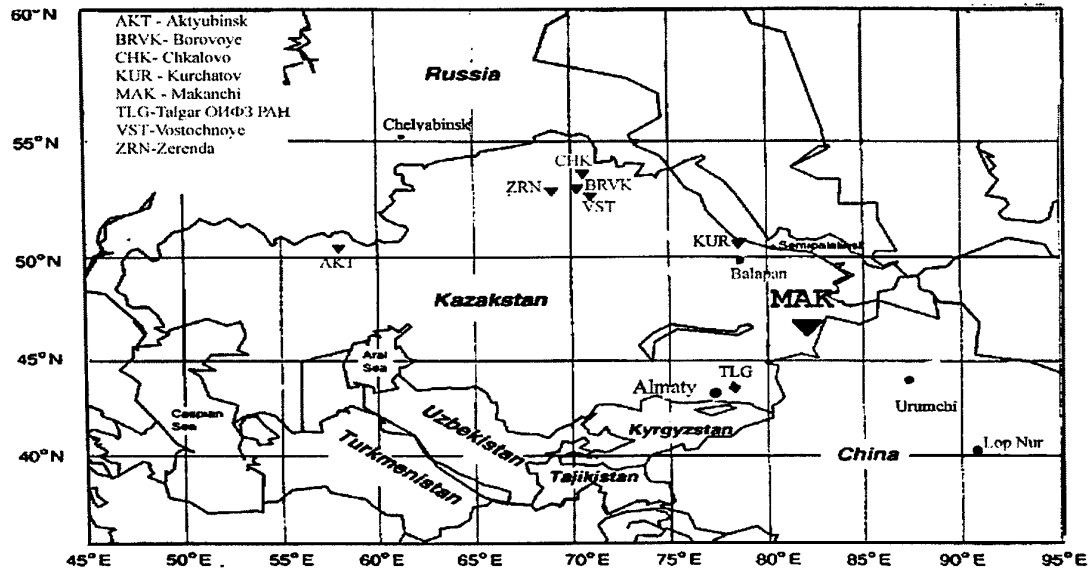


Figure 1. Locations of seismological stations of IGR NNC RK.

The Makanchi station is included in the Global Seismological Network (GSN), as well as it is one of primary stations of International Nuclear Monitoring System. From one hand, it's geographical location is very convenient for the monitoring of seismic events originated from the China's territory where underground nuclear explosions had been made (Lobnor nuclear test site is located in 700 km far from the station). From the other hand, the station is placed in seismological active region, where during the last ten years, the seismic activity is increased, which is seen by strong Zaisan earthquakes of 1990 year, with $M=6,9$ and $M=6,3$. Till the present time, no regular instrumental observations in this area have been made, published catalogues of earthquakes have no information about low seismicity of this area. So, seismological data from

Makanchi station is of great importance as for monitoring of underground nuclear explosions, as well as for monitoring of seismicity in the area of Djungarskii Alatau, Altai and other neighboring regions.

The main purpose of work under the contract was to investigate spectral characteristics of seismic background noise on the place of Makanchi station. The information about the noise level on different frequencies, its changes with time, its dependence from other factors, allow to judge about the sensitivity of the observational point to detect seismic events. And eventually, the knowledge of noise behavior on the place and usage of this knowledge during analysis of seismic signal, will allow to increase the effectiveness of station participation in nuclear monitoring.

1. Geographical location of Makanchi seismological station.

The Makanchi station is placed in the Eastern Kazakhstan. Its coordinates are: latitude – $46^{\circ}48'29''N$, longitude – $81^{\circ}58'37''E$, the elevation – 558 m. (Figure 2).

There is no railways and large cities near the seismic station. There is no drilling activity, no coal or other mines, no open casts. The single mineral resource enterprise (coal mining) is located near the Chuguchak city (China), in 70 kilometers away from the station.

The seismic station is located on the foot of Djaitobe mountain, in 5 kilometers to the north-west from Makanchi village, and connected to the village by a dirt road. There is a highway (Urdjar village - Bahty village - Chuguchak city (China)) with moderate traffic intensity, in 1,5 kilometers to the south-west from the station. There is a grader road to the east (about 4-5 kilometers) from the station, which connects Makanchi village and Blagodatnoe village (about 30 kilometers to the north from the Makanchi village). Also, there is a developed network of field dirt roads around the Djaitobe mountain, connecting small farms and settlements.

The Karasu river, which heads in the mountains of Tarbagatay ridge, and empties into Alakol lake, flows in 8-10 kilometers from the station. The river spreads to a width of 10 meters, with a depth up to 1 meter; on average, the width of the river is about 5-8 meters and depth is about 0,5-0,8 meters. The maximum of water level in the river is observed in April - May, during a spring snow melting. The Alakol lake is rather large, its surface is about 2100 square kilometers, and its depth is up to 20-25 meters. The lake is located in 50-70 kilometers to the south from the station. The Tarbagatay mountains are located in 40-50 kilometers to north from the seismic station. The station is located in the submountain valley of the Alakolskaya depression, where the

network of small rivulets is developed. Usually, these rivulets are dry in summer and are affluent only on springs.

2. Geological and tectonic description of the area of the Makanchi seismic station.

As it was mentioned above, Makanchi seismic station is located on the foot of Djaitobe mountain. The mountain is build up from the tuffs of acidic composition of Karkaralinskaya suite of Lower Carboniferous age (C_1V_3 - skr_2) and is a small outcrop of Paleozoic foundation among Quaternary deposits of Alakolskaya depression (Figure 3). The outcrops of rocks, belonging to Karkaralinskaya suite are observed, also, to the north from the Djaitobe mountain (the Kurtobe and Balatobe mountains), which are build up from tuffs of acidic composition too. The rocks of this suite expose also, at the south-east part of the area, where they consist of tuffs of acidic and middle composition of upper and lower members of Karkaralinskaya suite (C_1V_3 - skr_1 - C_1V_3 - skr_2). The thickness of deposits of this suite varies from 600 to 1100 meters.

On the north-eastern part of the area the small outcrops of tuffs of various composition of Upper Devonian age (D_3fm) are observed. The thickness of Famennian deposits reaches 900-1000 meters.

On the south-eastern part of the area, in Kyzylshaly mountains, the outcrops of medium-grained biotite alaskaite subalcalic granites, aplitic subalcalic granites and granite-porphyrites, usual for endocontact facie, are observed. This granitoid massif breaches lower-carboniferous and upper-Devonian deposits (outside the limits of described area), and is dated as late-upper-Paleozoic (γPz_3III) complex of granitoids.

The area, adjoining the station, is overlaid with loessal sandy loams, proluvium-deluvial adoles with gravel, sands, coarse gravel, boulders, clays, silts of middle-upper-modern age of Quaternary period. The thickness of Quaternary deposits is from 20 up to 100-150 meters.

The site of Makanchi station is located in the Alakolskaya depression, which is a young structure formation of the second order of the large Balhashskaya (Djungaro-Balhashskaya) hercynian geosyncline, and adjoins on the north to the Tarbagataiskii anticlinorium [1,2]. The extensively developed Cenozoic deposits don't allow completely reconstruct a structure of folded formations of Paleozoic basement of this structure.

The comparison of results of geological mapping with data, obtained on the base of geophysical survey (at a scale of 1:200 000) carried out in this area, allowed to find here two large

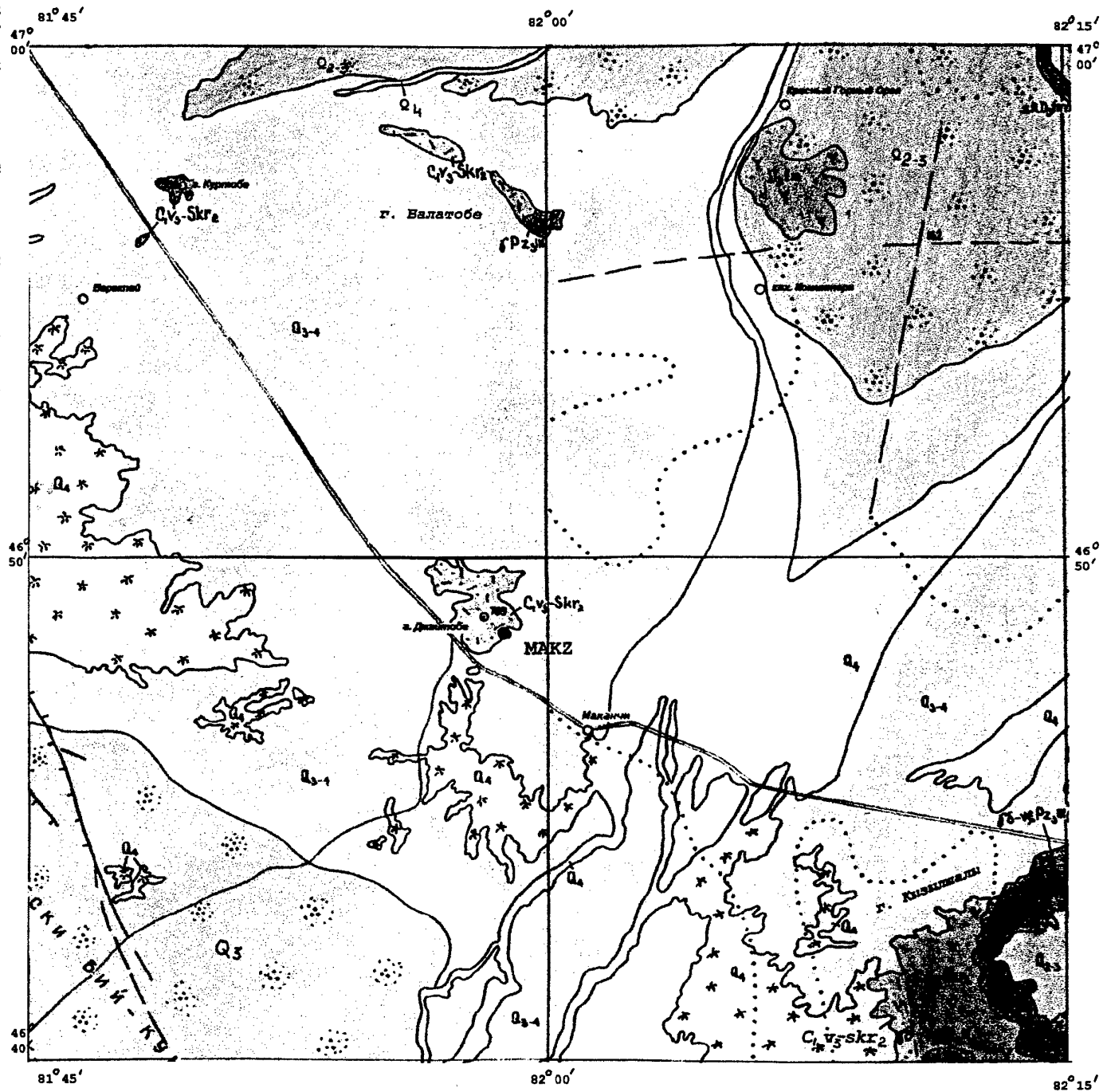


Figure 3. Geological map of the area of the "Makanchi" seismic station.
Scale 1:200000

EXPLANATION

for geological map

QUATERNARY SYSTEM

-  Recent group. Boulders, shingles, sands, sandy loams, loams, clays, silts. Swamp and lake -swamp loams
-  Upper and recent groups. Boulders, shingles, debris sandy loams and loams, sands, sandy loams, loams
-  Upper group. Sands, lake and lake -alluvial sandy loams, loams and silts
-  Middle and upper groups. Loess-like loam and sandy loams, and proluvial-deluvial loams with debris

CARBONIFEROUS SYSTEM

-  Lower group. Upper Visean substage – Serpukhovian stage. Karkaralinskaya suite. Upper member. Andesitic porphyrites, trachyliparitic porphyrites, tuffs sour and alkali-type effusive rock, tuffconglomerates, tuffsandstones
-  Lower group. Upper Visean substage - Serpukhovian stage. Karkaralinskaya suite. Lower member. The tuffs of middle composition and andesitic porphyrites, tuffbreccias, quartzless porphyrites

DEVONIAN SYSTEM

-  Upper group. Famennian stage. Porphyrites sour and middle composition, tuffs, tuffconglomerates, limestones

INTRUSIVE FORMATIONS

UPPER PALEOZOIC INTRUSIONS

-  Late upper paleozoic complex of granitoids. Inequigranular leucocratic, alaskaite, subcalic granites and granite-porphyrites (γ), granodiorites (γδ), quartz-diorites and diorites (δ), quartz-monzonites (vξ), syenites
-  The blue caps of contacting metamorphism

FACIAL VARIETY OF INTRUSIVE FORMATIONS

-  Granites, granite-porphyrites
-  Granodiorites, quartz-diorites and diorites, quartz-monzonites, syenites, adamellites, tonalits, gabbro

VOLCANOGENIC FORMATIONS

-  Acidic composition, essentially tuffs
-  Middle composition, essentially tuffs
-  Different composition, essentially tuffs

QUATERNARY FORMATIONS

	River, deluvially-proluvial, alluvially- proluvial
λ λ	Alkaline eapth
••••	Eolian

OTHER NOTATIONS

••••	The borderline of granitic massifs, plotting as to geophysical this
/	Borderline normal stratigraphic and intrusive contact reliable
- - -	Borderline normal stratigraphic and intrusive contact intended
••••	The borderline of facies
/	The line of tectonic contact reliable
- - -	The line of tectonic contact intended
/	The line of tectonic contact reliable with instruction the courses of surface crust displacement
- - -	The line of tectonic contact intended with instruction the courses of surface crust displacement
- - -	The line of tectonic contact plotting as to geophysical this

Stratigraphic column

System	Group	Stage	Index		Thick-ness, m	Rocks characteristics
Quaternary	Recent		Q ₄		2-12	Boulders, shingles, sands, sandy loams, loams, clays, silts. Swamp and lake-swamp loams
	Upper-Recent		Q ₃₋₄		10-20	Boulders, shingles, debris sandy loams and loams, sands, sandy loams, loams
	Upper		Q ₃		10->100	Sands, boulders, shingles
Quaternary	Middle-Upper		Q ₂₋₃		50->100	Jonquil-yellow loess-like loam with fauna: Zonitoides nitidus Mull., Fruticicola striotula cpl., Eulota fruticum Mull., Vallonia tenuilabris A. Braun, Cochlicopa lubrica Mull., Galba truncatula Mull., Euomphalia rubens Mart., Subzebrinus labiellus Mart. Loess-like sandy loam, proluvial-deluvial loams with debris
Carboniferous	Lower	Visean - Serpukhovian	C _{1v3} -skr ₂		600-900	Karkaralinskaya suite. Upper member. Andesitic porphyrites, their tuffs with the horizons of orthophyres, of quartzless porphyrites, of tuffs and ignimbrites, of the tuffs of trachyliparitic composition, the lenses of sandstones and aleurolites. Aleurolites with Mesocolamites ramifer (Stur/) Hirn. Tuffconglomerates, tuffbreccia, tuffs acidic alkali-type effusive rock
			C _{1v3} -skr ₁		1100	Karkaralinskaya suite. Lower member. The tuffs of intermediate composition and andesitic porphyrites, quartzless porphyrites, tuffs mixed composition, the lenses of sandstones and aleurolites with flora Angaropteridium abacanum Zal., Angaropteridium cardiopteroides (Schmal.) Zal.
Devonian	Upper	Famenian	D ₃ fm		900-1000	Andesitic porphyrites, dacitic porphyrites, tuffs, tuffconglomerates, the rare blankets of diabases, organogenous boulders, conglomerates, gritstones. Fauna: Cyrtospirifer sulcifer Hall et Clark, Cyrtospirifer semisbugensis Nal., Cyrtospirifer platynotus Nal. Non Weller

zones – eastern and western ones. These zones differ in the directions and amplitudes of movements, occurred here during Cenozoic age. The border of zones has a north-western direction, and roughly coincides with the bottoms of Urdjar and Egin-Su rivers, to the west from the described area.

The Makanchi seismic station is located in the eastern zone, with relatively shallow attitude of Paleozoic basement, outcropping in several places out of overlaying Cenozoic deposits (Djaitobe, Kurtobe, Balatobe mountains on the northern part, and Akirek, Kyzzykshaky mountains on the south-eastern part).

The allotments of folded formations of Hercynian structural stage, and superimposed on it low-angle and horizontal Cenozoic formations of Alpine structural stage are found here.

The folded formations of Paleozoic basement can be studied only on rather small disembodied sites, and it is not possible to reconstruct the whole schema. The rocks of middle Devonian and lower Carboniferous period, participating in the folding, have as a rule, a north-western direction. Their angle of incidence is, in average, $50-60^\circ$, though, bigger angles were observed (up to $70-80^\circ$).

The results of electric sounding showed, that on the most part of the zone, the Paleozoic basement occurs at the depths of several dozens of meters, with a gradual subsidence in the south-eastern direction. The central part of the zone is featured by the shallow depression, placed between Karpebay mountain (outside the western border of the map) and Djaitobe and Kurtobe mountains. The depression has a north-western direction, and is traced at the length of about 60 kilometers, having a width about 10-12 kilometers. The depth of occurrence of basement here is 100-150 meters.

The small ruptured rock disturbances are, as a rule, a branch fissures of bigger faults, which control the formation of tectonic structures. We don't have precise data about absolute age of these faults. It seems, most part of the faults aroused in before-Silurian and Silurian age, and was rejuvenated in several steps during subsequent development. The faults have mainly north-western direction, and traced on big distances. As a rule these faults mark the borders of tectonic zones. These faults spread out of limits of described area. The first fault is Ayaguzsko-Urdjarskii fault, which is a regional fault, it spreads on a big distance from the north-west to the south-east and connects formations of various ages. It has rather big amplitude of displacement (about several kilometers) and it divides such structures, as Tarbagataiskii anticlinorium and Alakolskaya depression in the 40-50 kilometers to the north from Makanchi seismic station.

The second fault is Kyzyl-Beldeyskii fault, it is located in 16-18 kilometers to the west and south-west from Djaitobe mountain. This fault is a branch of the first fault and has a smaller amplitude of displacement. The fault is located outside the borders of described area, and stretches far from the given area (more than 100 kilometers).

All faults are featured by the straight strikes and heavy pitches of slip planes.

3. A description of seismological equipment, installed on the station.

During 1994 - 1996 yy seismic station PASSCAL had been operated in Makanchi. In October, 1996 station IRIS-2 GSN was installed on a place of PASSCAL station. The IRIS-2 GSN station is in operation for the present time.

The seismometers on Makanchi station are placed in a vault at a depth of about 10 meters from a ground surface. The length of the vault is about 20 meters. Seismometers are fixed on a concrete plinth, the size of the plinth is about 1,5 by 3 meters, and it's height is about 1 meter. There are three seismometers in the IRIS-2 GSN station: STS-1, STS-2 and accelerometer FBA-23. The most fundamental goal for the GSN system is to record the entire signal spectrum from teleseismic events of any magnitude in a single continuously recorded broadband channel. So, the basic IRIS-2 VBB channel records events with a frequencies starting from 0,1 second and up to 100 000 seconds. The IRIS-2 VBB channel has very large dynamic range - 138 dB. Despite the unprecedented bandwidth and dynamic range of the IRIS-2 VBB channels, the broadband records will not capture the entire signal spectrum that includes high-frequency signals (above 7 Hz) or strong ground motion. Therefore, the very-short-period (VSP) channels of STS-2 seismometer and low-gain (LG) channels of FBA-23 accelerometer are in operation on the station.

The instrument responses of all three seismometers are shown on the Figure 4.

The long-period (LP), very-long-period (VLP) and ultra-long-period (ULP) channels also operate in the system. These channels are extracted from the VBB channels by filtration (weighted averaging using low-pass filtering) and decimation of data samples.

Also, there is a number of auxiliary channels in the IRIS-2 GSN system.

The parameters of main channels of Makanchi station system are given in Table 1.

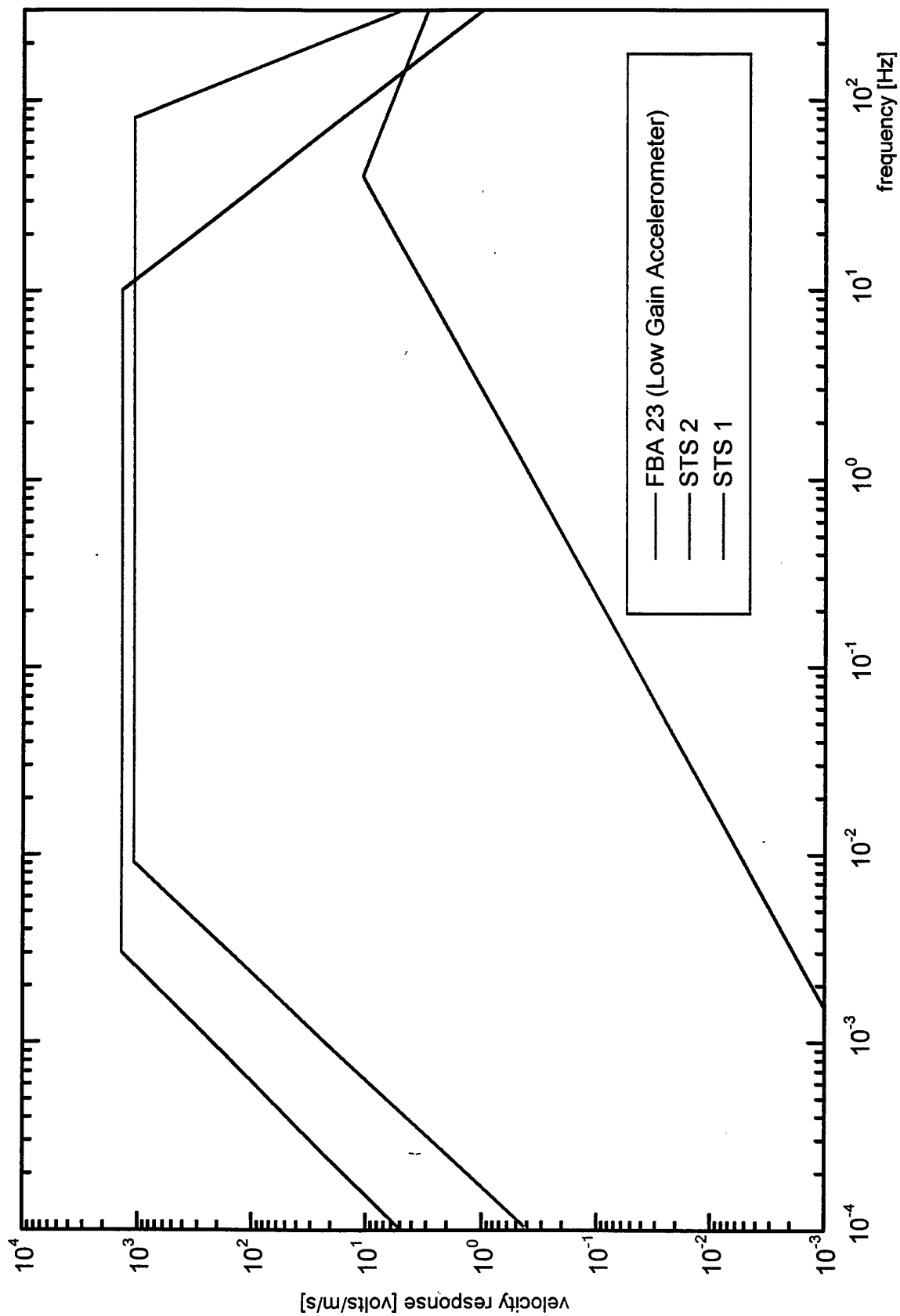


Figure 4. Velocity Response Comparison of IRIS/USGS GSN Instruments.

Table 1.

Parameters of main seismic channels of Makanchi station.

CMP STREAM	SAMPLING RATE	SEISMOMETER	DATA	REMARKS
VSP	80 Hz	STS-2	events	VSP
SSP	40 Hz	STS-2	continuous	VSP
VBB	20 Hz	STS-1	continuous+events	VBB
LP	1 Hz	STS-1	continuous+events	derived from VBB
VLP	0.1 Hz	STS-1	continuous+events	derived from VBB
ULP	0.01 Hz	STS-1	continuous	derived from VBB
LLG	80 Hz	FBA-23	events	low-gain (LG)
LLP	1 Hz	FBA-23	continuous	low-gain (LG)

Each channel records data by three components: one vertical component (Z) and two horizontal components, with orientation north-south (N) and west-east (E).

4. Data selection and data processing.

The records of channels SSP, VBB, LP and VLP, recorded during October 1996 - December 1997 (see Table 2) were used in the present work. It necessary to note, that because of errors in software operated on Makanchi IRIS-2 GSN station, the overflow of data buffers occurred almost every day, so, the length of continuous record for different channels varied from several minutes up to 12 - 16 hours. The error in software was corrected in June 1997. So, the VLP data were taken only from the second half of 1997. For VLP channels the following four records with a length of several days each were selected (in format ddd:hh): 282:20 – 286:12, 274:00 – 276:03, 232:17 – 235:18, 250:12 – 253:10.

Also, there was a lot of problems with STS-2 seismometer. Starting from November 1996, the channels of STS-2 seismometer became very noisy (instrumental noise) and in May 1997 the seismometer was out of order completely. In November 1997 the STS-2 seismometer was repaired. So, as it is seen from the table, for SSP channels we have only autumn's data.

The noise spectra were calculated for all three components of each channel.

Even at the phase of preliminary visual analysis, the clear difference between day and night records was visible. The horizontal components during local day time have intensive long-period oscillations (see Figure 5). So, after that, noise spectra were calculated separately for day and for night. The main requirement for the selection of records was the absence of seismic events and

the absence of 'tails' of preceding strong events. We scanned all available data for LP channels, and all records, meeting the mentioned above requirements (the absence of events and the length not less than 7 hours) were selected. After that, for selected by LP channel time records, the VBB and SSP channels were scanned, and records with a length of 1 hour for VBB channels and 0,5 hour for SSP channels were selected, free from minor high-frequency events and instrumental outbursts.

The computation of power spectral density was carried out in accordance with technique provided in [3, c 425-430]. There were the following steps during data processing:

- 1) data were differentiated, in order to obtain the acceleration records
- 2) each selected record was divided on a number of overlapping segments with a size of 8192 samples (that corresponds to, roughly, 7 minutes for VBB channel and 2,5 hours for LP channel). The segments were overlapped by 50%. Fast Fourier transform was applied to each segment and spectral estimates for all segments of given record were averaged.
- 3) The instrument response was removed, using data from the header of records.
- 4) At last, five-point smoothing was applied.

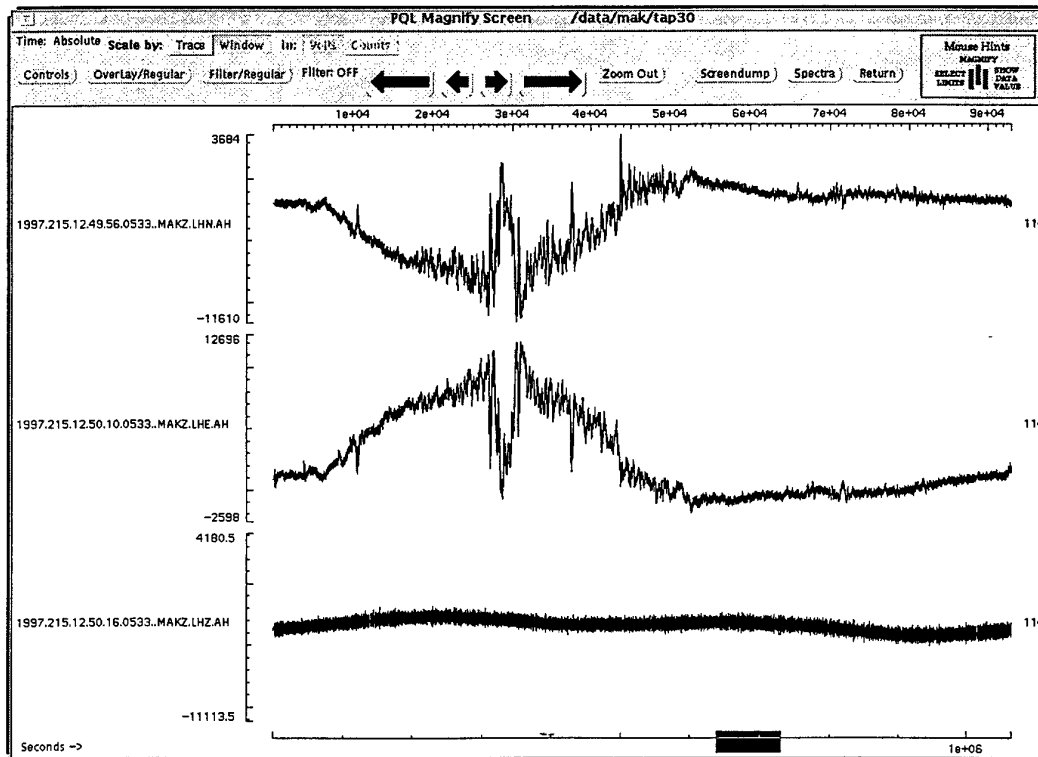


Figure 5. The typical example of initial record. The length of record is 24 hours. The beginning of record correspond to the 6 hours of local time. Components from up to bottom: north-south, east-west, vertical.

As a result, for each channel the power spectral density of seismic noise was computed in the following periods:

SSP channel : 0,05 - 200 seconds;

VBB channel: 0,1 - 400 seconds;

LP channel: 2 - 8000 seconds;

VLP channel: 20 - 80 000 seconds.

Table 2.

Times of records, used in the computation of seismic noise

	DAY			HIGHT		
	VBB	LP	SSP	VBB	LP	SSP
1996 October	6 291:04** 293:04 293:06 297:07 298:05 298:09	4 291:01 293:01 297:04 298:01	3 297:07 298:05 298:09	9 289:16 289:22 294:16 294:21 295:15 295:21 297:20 303:14 303:20	5 289:16 294:13 295:13 297:17 303:13	9 289:17 289:22 294:16 294:21 295:15 295:21 297:20 303:14 303:20
1996 November	6 309:10 310:03 321:03 323:09 324:04 329:02	6 309:06 310:01 321:01 323:01 324:01 329:01	2 309:10 310:03	8 308:13 308:18 318:16 321:18 323:16 327:20 328:19 330:22	7 308:13 318:15 321:12 323:14 327:17 328:13 330:13	2 308:13 308:18
1996 December						
1997 January						
1997 February						
1997 March	2 086:03 087:04	2 086:01 087:01				
1997 April	2 100:08 107:02	2 100:06 107:02	1 100:08	5 090:16 099:21 100:20 107:18 109:20	5 090:14 099:16 100:15 107:14 109:17	2 099:21 100:20
1997 May	4 132:08 139:08 140:06 141:04	4 132:01 139:05 140:05 141:01		3 132:19 139:22 142:18	3 132:17 139:15 142:16	
1997 June	2 152:05	2 152:01		1 164:15	1 164:13	

	158:05	158:01				
1997 July	2 185:08 186:06	2 185:01 186:03		2 183:17 188:16	2 183:13 188:15	
1997 August	4 223:04 230:07 233:04 235:09	4 223:0123 0:01 233:01 235:00		8 219:19 220:17 225:21 228:17 231:20 233:18 234:10 242:18	8 219:13 220:12 225:15 228:13 231:13 233:13 234:13 242:13	
1997 September	6 245:06 254:04 255:06 257:07 259:03 265:04	6 245:01 254:01 255:01 257:03 259:01 265:01		3 244:19 245:21 256:17	3 244:15 245:15 256:15	
1997 October	5 274:05 275:05 283:08 286:05 287:05	5 274:03 275:01 283:02 286:02 287:01		4 274:14 275:15 285:17 289:17	4 274:13 275:13 285:14 289:13	
1997 November	3 314:06 316:11 328:05	3 314:02 316:07 328:04	4 314:03 314:08 316:11 328:05	5 311:20 321:22 325:14 326:21 333:22	5 311:19 321:13 325:13 326:13 333:16	9 325:13 325:21 326:21 333:22 311:20 311:23 321:18 321:22
1997 December	7 335:07 336:06 353:06 354:08 359:03 362:09 363:09	7 335:03 336:01 353:02 354:02 359:01 362:05 363:01	2 335:07 336:06	6 337:20 353:14 360:17 361:13 362:17 364:20	6 337:15 353:14 360:13 361:13 362:13 364:15	1 337:20

* - the number of records, used in given month

** - day and hour, corresponding to the beginning of the given record.

5. The analysis of background seismic noise.

The generalized seismic noise spectra for the diapason, covering more than six orders from $6 \cdot 10^{-2}$ sec up to 105 sec for all three components are shown on the Figure 6. Looking on this spectra it is possible to analyze the main characteristics of seismic noise near Makanchi seismic station. As it's seen, for the periods below 20 sec the curves for vertical and both horizontal components are close to each other – divergence between them is not more than 5-7 dB. In the

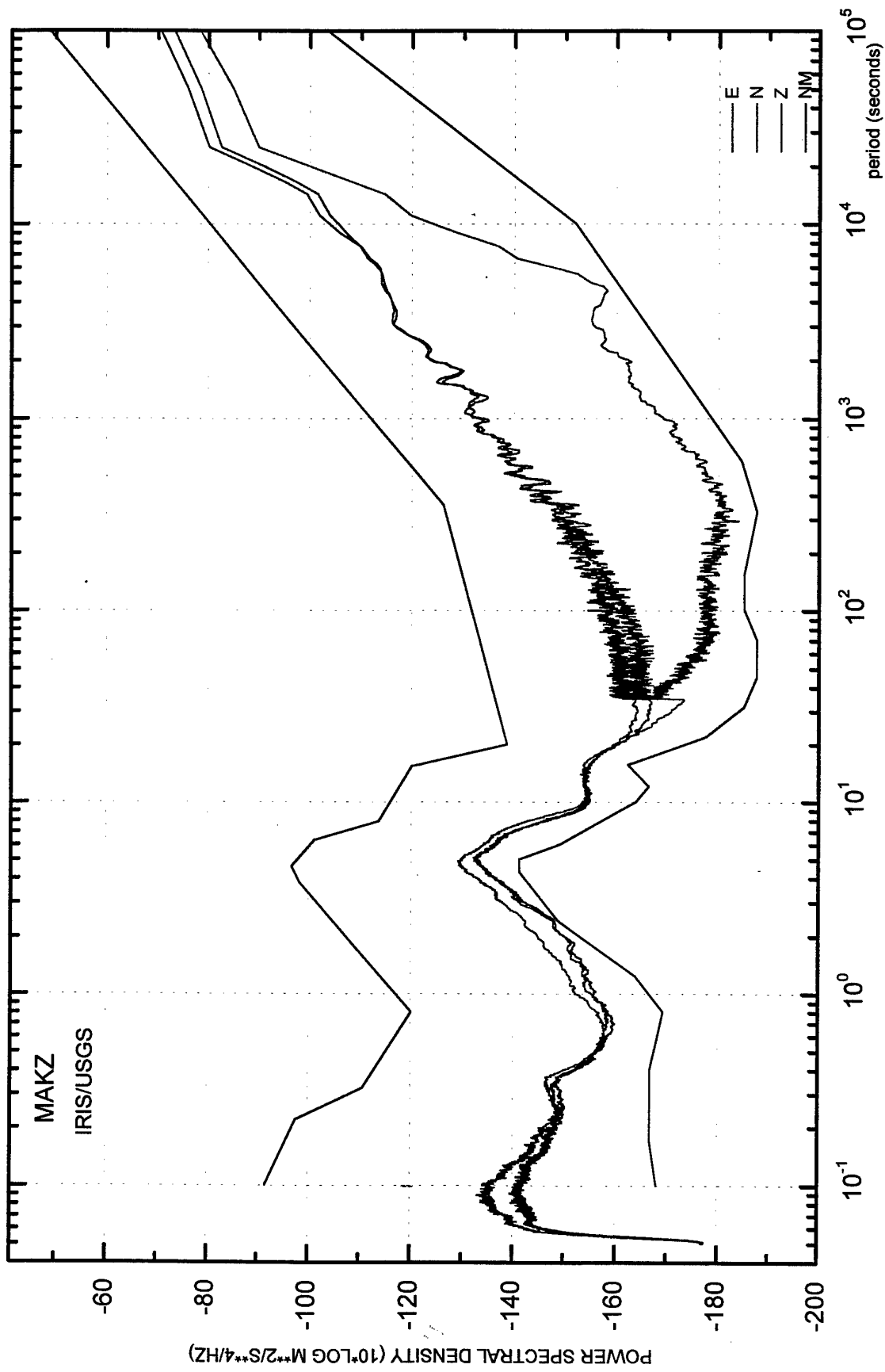


Figure 6. Noise spectra for Makanchi station, containing SSP, VBB, LP and VLP data.

long-period part of spectra ($T > 20$ sec) the significant difference between components is observed. The noise spectrum for Z-component is the quietest one among all components for long periods. This conclusion is in accordance with results for other GSN seismic stations [4].

The noise spectra computed for Makanchi station were compared with New Noise Model [4]. Upper and lower border of new model of seismic noise are marked on Figure 6 by solid lines. The main extremums, found on a new noise model, are seen on the Makanchi noise spectra too: the oscillations with periods 5 sec and 18 sec. This oscillations are aroused because of natural microseismicity of Earth, and they are recorded in any part of the Earth globe.

The local maximum at the period 0,35 sec is found on Makanchi noise spectra. This maximum, apparently, is associated with industrial noise, and is specific for this station. This maximum became stronger during day time, and became weaker during nights. For the periods 0,5 sec – 20 sec noise spectra for Makanchi station lies close to the low noise model; and it is very important, since the sensitivity of station in these periods, to a great degree, determines the effectiveness of monitoring of regional events.

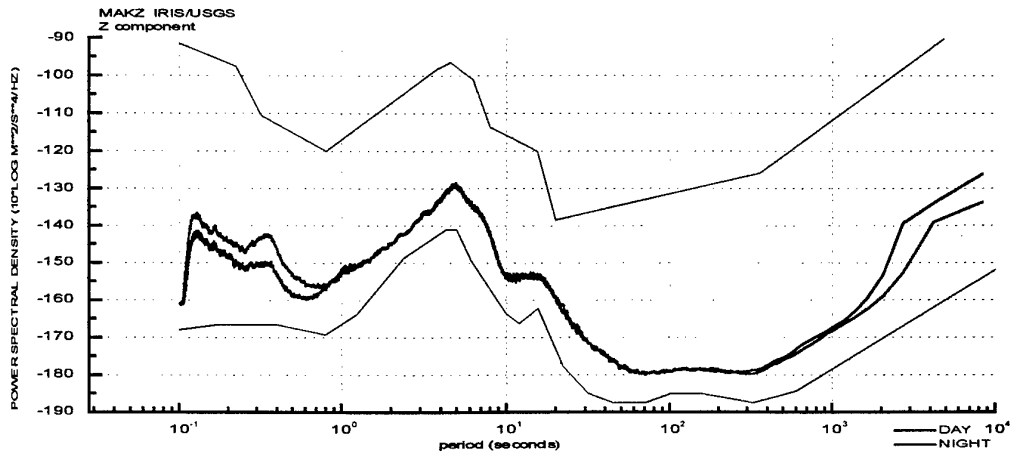
The comparison of noise spectra for Maknchi station with noise spectra from two neighboring IRIS stations Ala-Archa in Kyrgyzstan and Urumchi and China, located in the Tian-Shan, was made. The instruments on all three station are the same, and are installed on bedrocks.

Generally, for the periods less than 20 sec, all three station give spectra close to each other. In the high frequencies (> 10 Hz) Makanchi looks worse than Ala-Archa, but significantly better than Urumchi. There is no arise of noise level for the period 1,6 sec, which is clearly visible on all three components of Ala-Archa station, and occurs because of storm winds on Issyk-Kul lake. For this period the noise level on Makanchi is on 10 dB less.

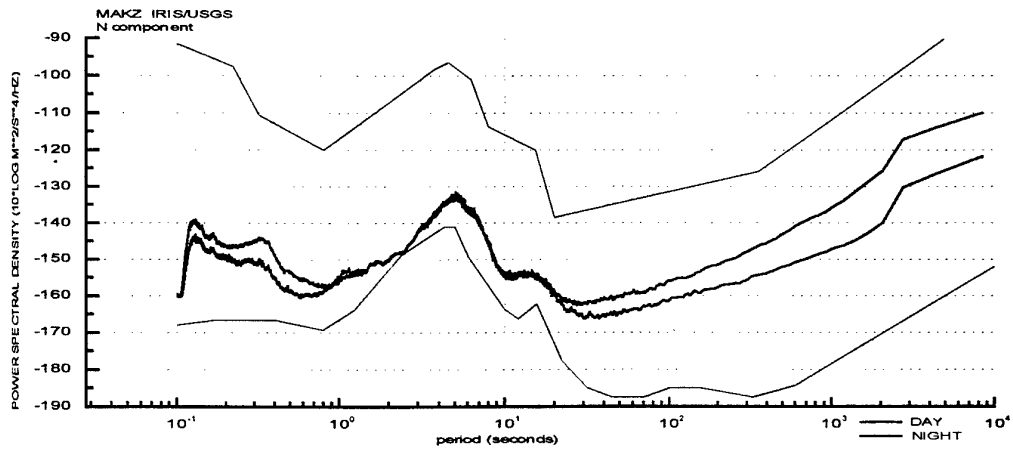
For the long-period part, Makanchi station noise spectra look worse than spectra from Ala-Archa and Urumchi stations. It occurs because of long-period waves on horizontal components during day time (Figure 5).

Comparison of day and night noise spectra. The noise spectra were computed separately for day and night time periods, in order to make a detailed study of variations of seismic noise level influenced by natural and industrial disturbances. Day records comprise times from 7 a.m. till 7 p.m. The night records, accordingly – from 7 p.m. till 7 a.m. The comparison of day and night noise spectra by all three components is shown on Figure 7.

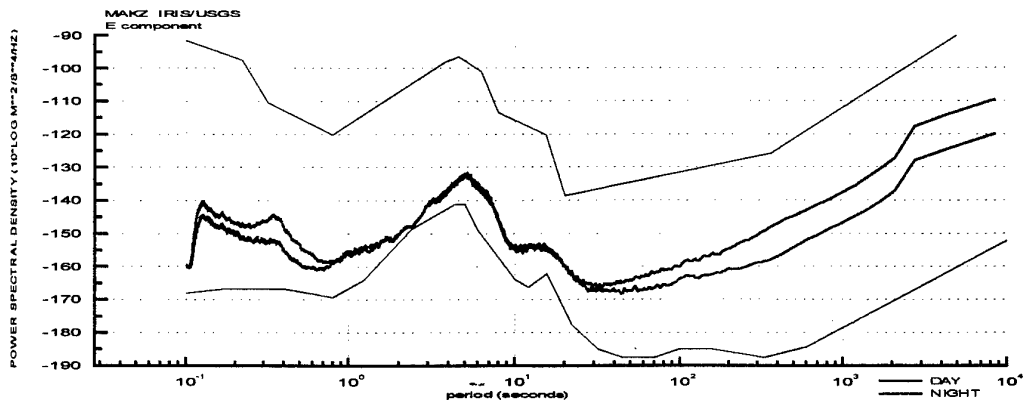
The following regularities are found. The station's sensitivity for vertical component (Figure 7a) decreases during day time in the high-frequency band (from 0,14 to 0,8 sec) and in the very



a)



b)



c)

Figure 7. Comparison of day and night medians of seismic noise
 a) Z component, b) N component, c) E component.

long period band ($T > 1000$ sec). For other periods there is no significant difference between day and night noise spectra for vertical component.

On horizontal components the increase of noise level in high-frequency band (similar to vertical component) is clearly visible. But, besides this, for both horizontal components, there is observed an increase on 5-10 dB of noise level for periods longer than 20 sec for day spectra against night spectra.

The increase of noise level during day time for periods 0,3 - 0,35 sec, is clearly visible on all three components, which is evidently caused by local industrial (artificial) activity.

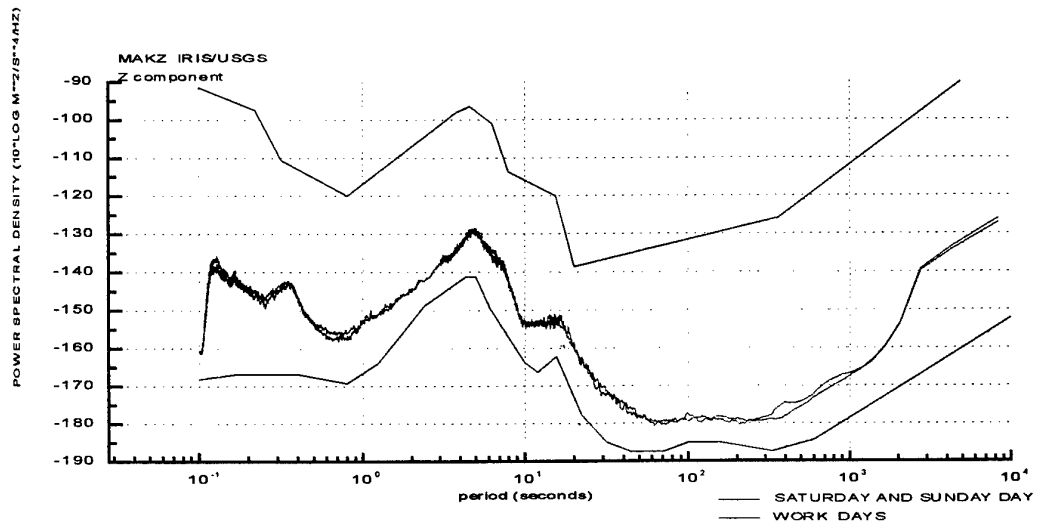
The comparison of work days against week-end days. The comparison of noise spectra, created from records of work days, against noise spectra, created from Saturdays and Sundays days have been made (see Figure 8). There is almost no difference between these noise spectra.

The study of seismic noise variations during a whole day and between winter and summer day. Two records with a length 24 hours each, of two quiet days were selected: summer day 22.08.97 (234) and winter day 29.12.97 (363). The noise spectra were computed by VBB channel for each hour of both days (24 noise spectra for each day). After that, the whole period was divided onto seven parts: 0,14-0,3 sec, 0,3-1 sec, 1-3 sec, 3-10 sec, 10-30 sec, 30-100 sec and 100 - 400 sec (Figures 9-16). And for every hourly noise spectra for every of seven bands the average value was computed. So, each point on Figures 9-16 is an average of given hourly spectra by given period.

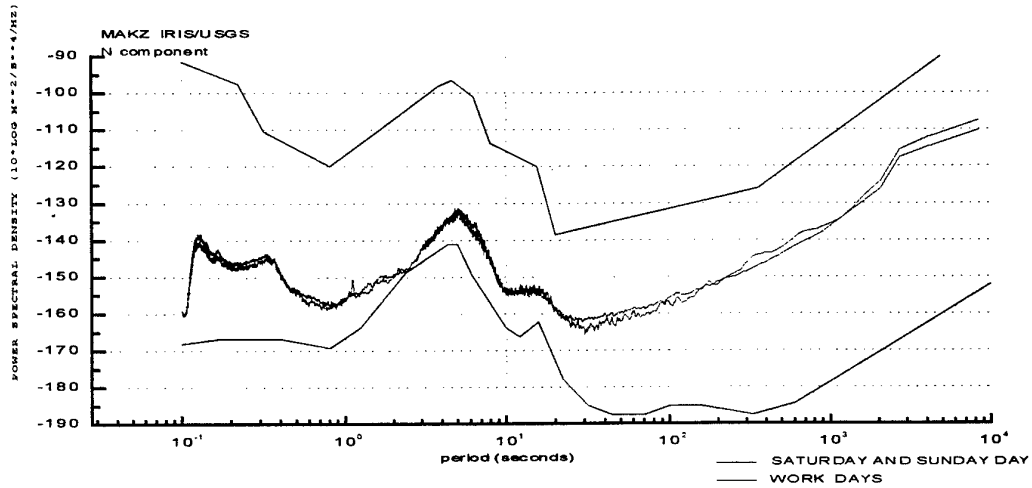
For periods 0,14-0,3 sec and 0,3-1 sec (Figures 9 and 10) the daily variations are clearly visible. For winter day there is the following rule: the lowest noise level is during night time (0-6 hours), the highest noise level is during day time (7-16 hours). After 16 hours begins the gradual decrease of noise level. The picture is similar for all three components. The noise level changes here on 16 dB.

For summer day the noise level for these two periods is higher during all the day. But it's behavior differs from the winter day. The noise level at night for summer day is the lowest too. But, if during the winter day the noise level decreases after 16 hours, the noise level for summer day stays high up to 22-23 hours.

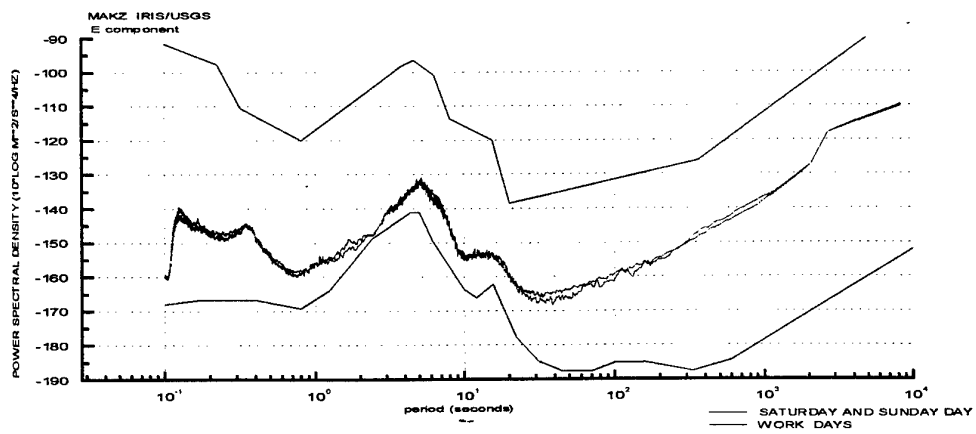
For longer periods, the daily variations of noise level decrease and disappear at all. For periods 1-3 sec, 3-10 sec (Figures 11, 12), there is almost no variations, especially for winter day. For the period 3-10 sec, the relative level of noise is reversed: for all three component winter day has higher noise level (6 dB) during all 24 hours, than summer day. For the period 10-30 sec (Figure 13) the noise level for winter day is higher, than that for the summer day, too. For period 30-100 sec (Figure 14), the noise levels for both days are almost the same. For period 100-400 sec



a)



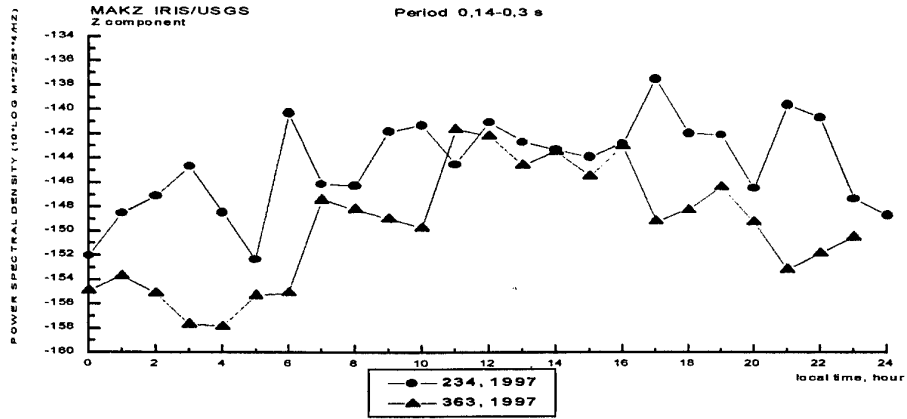
b)



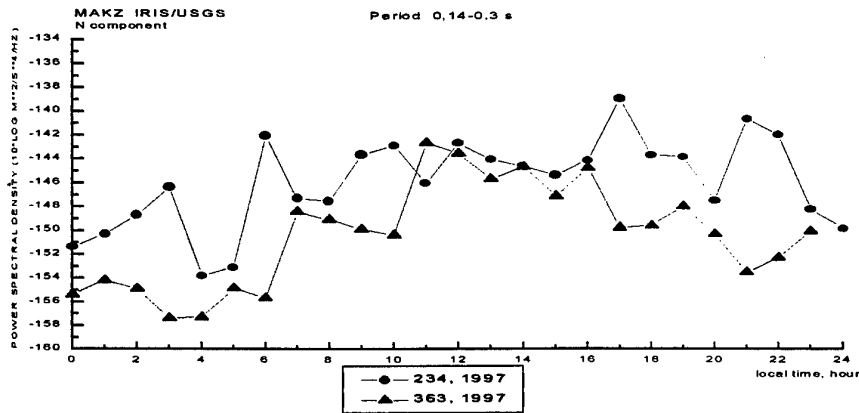
c)

Figure 8. Comparison of medians of seismic noise for work days and for week-end days.

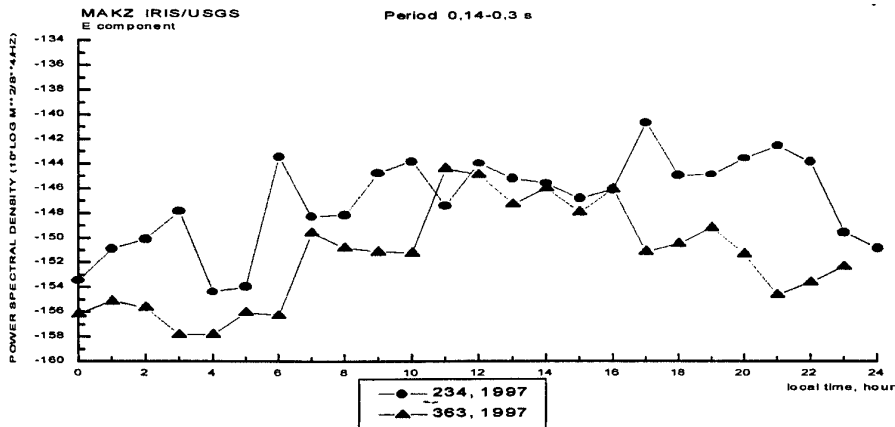
a) Z component, b) N component, c) E component.



a)

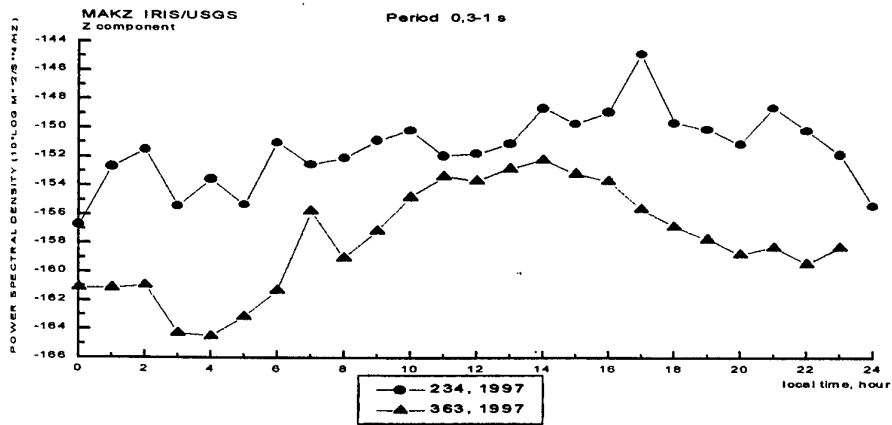


b)

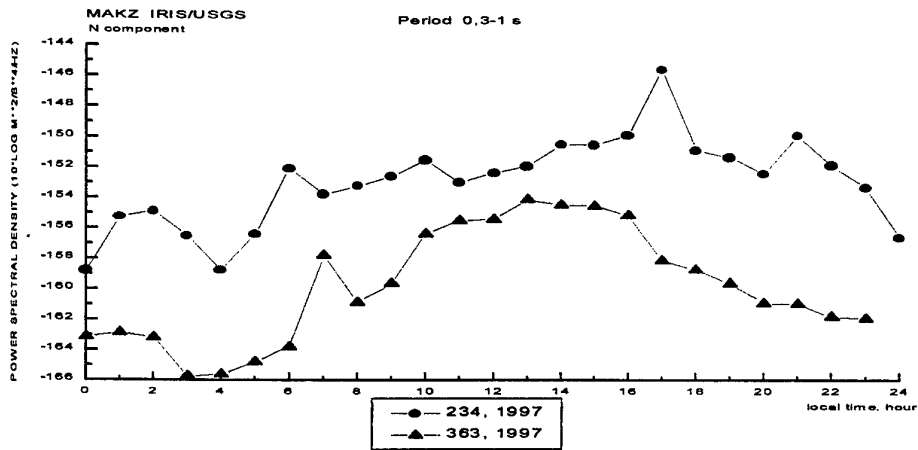


c)

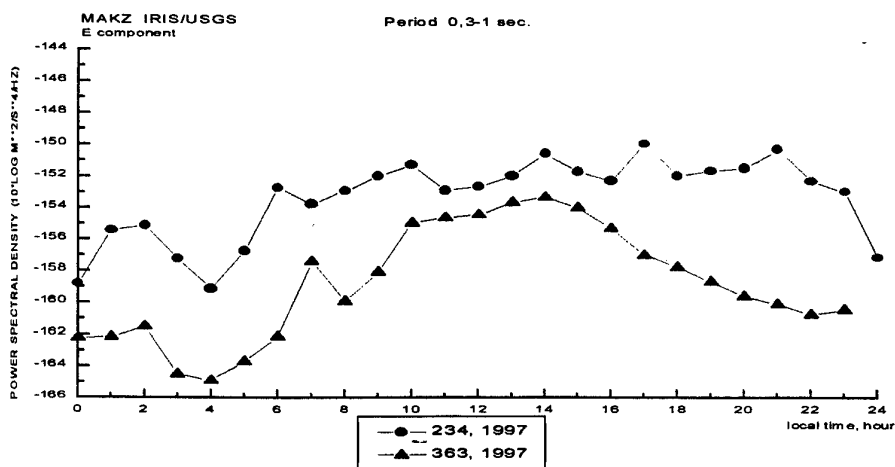
Figure 9. Variations of seismic noise during a day for the period of 0.14-0.3s.
a) Z components, b) N components, c) E components



a)

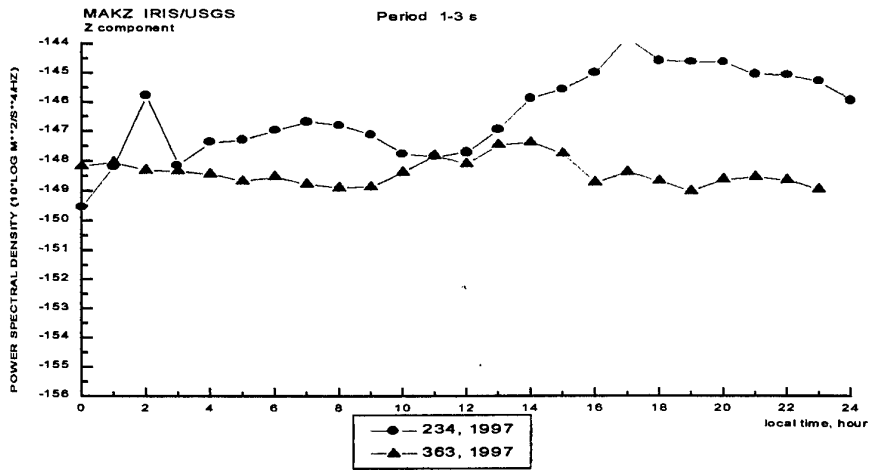


b)

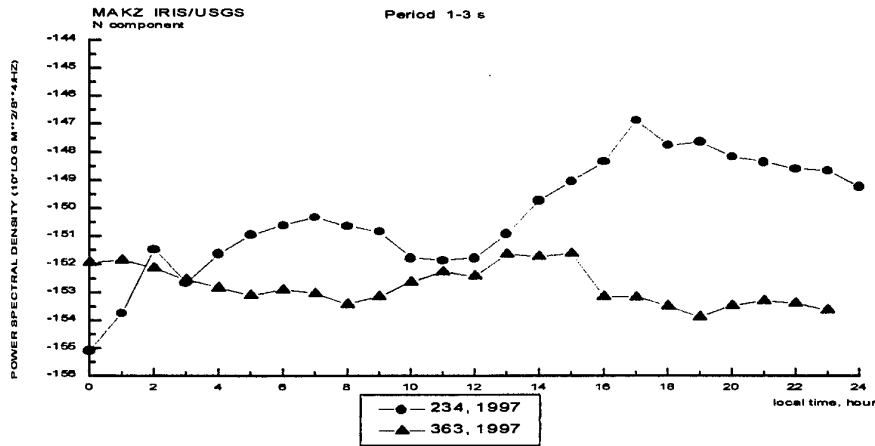


c)

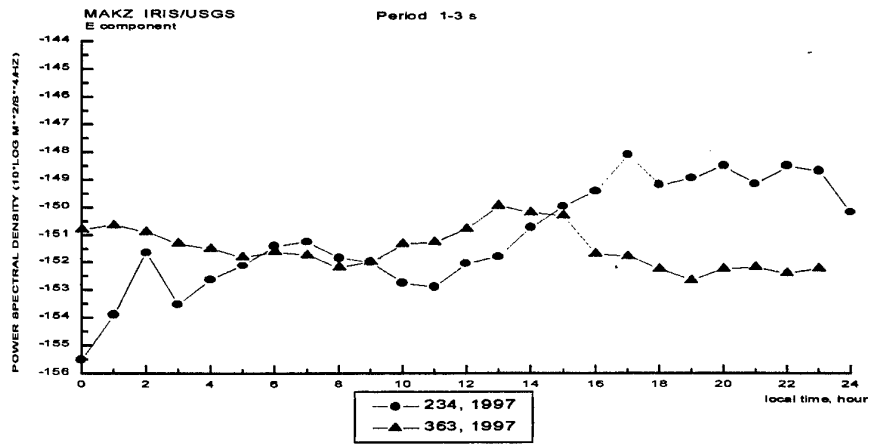
Figure 10. Variations of seismic noise during a day for the period of 0.3-1s.
a) Z components, b) N components, c) E components



a)

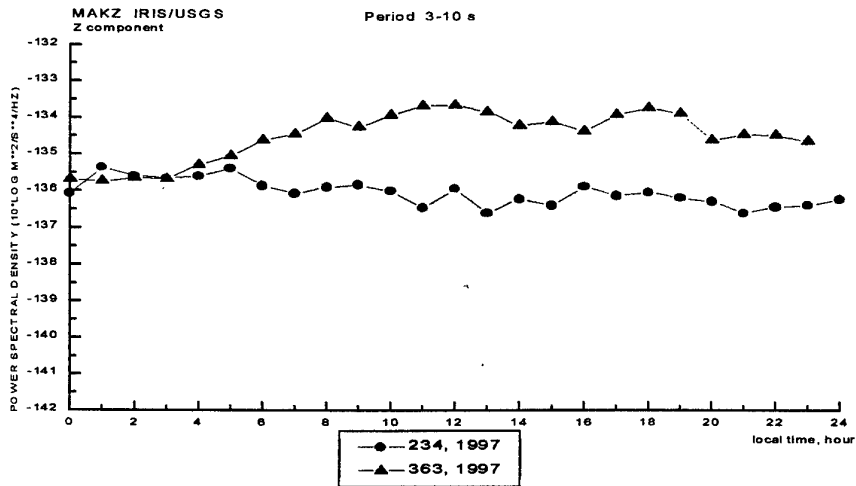


b)

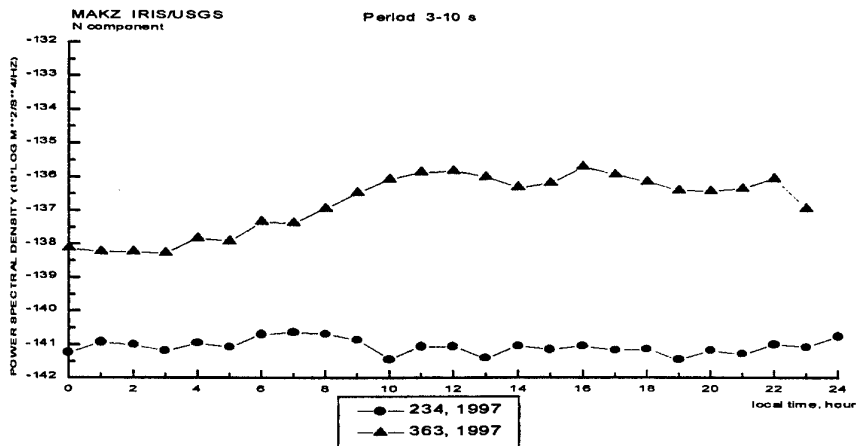


c)

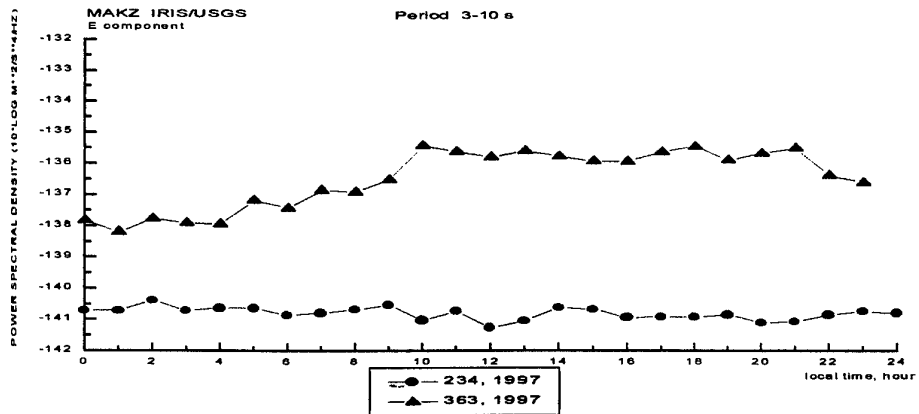
Figure 11. Variations of seismic noise during a day for the period of 1-3s.
a) Z components, b) N components, c) E components



a)

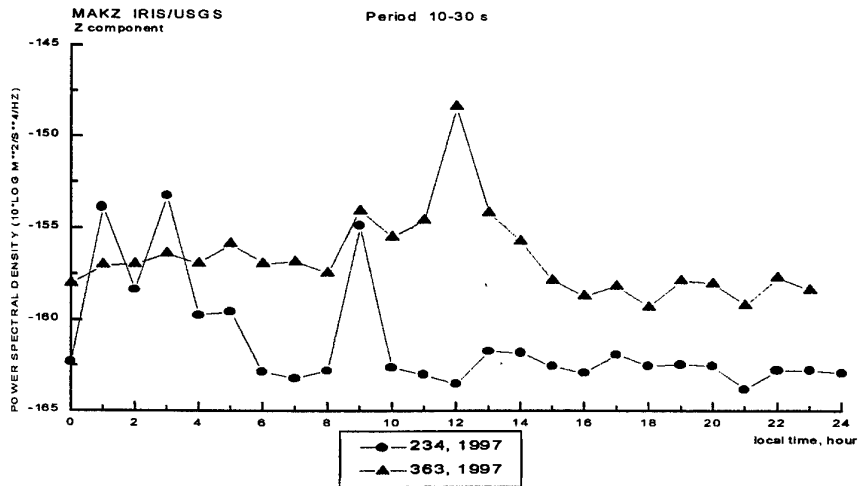


b)

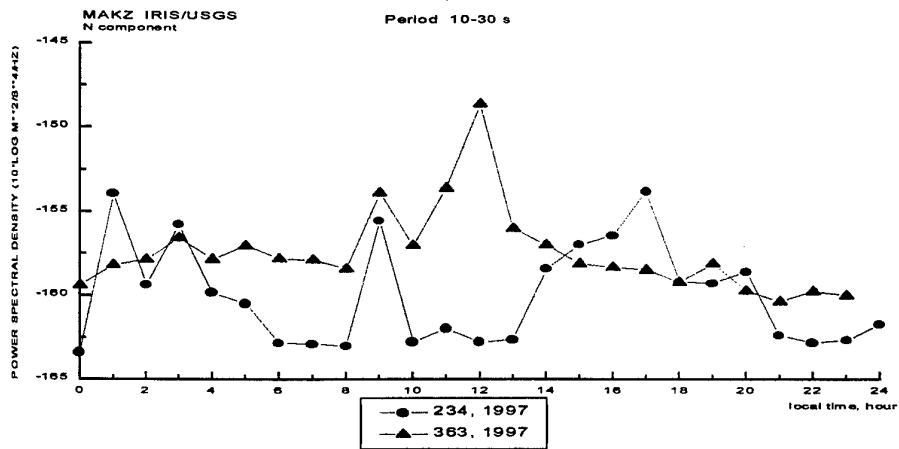


c)

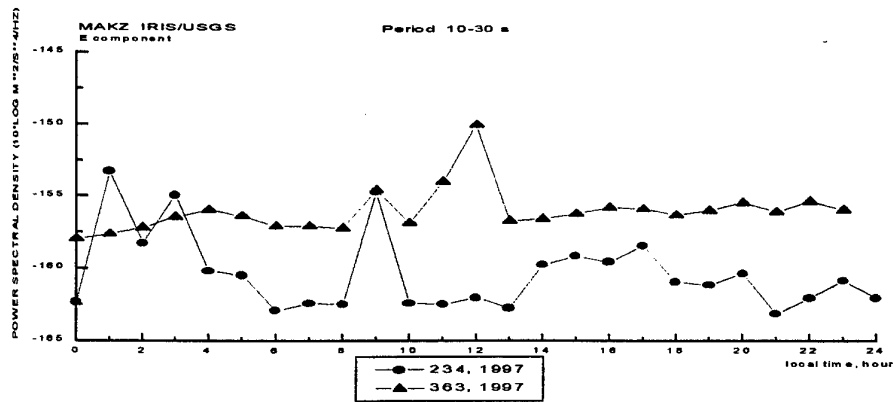
Figure 12. Variations of seismic noise during a day for the period of 3-10s.
a) Z components, b) N components, c) E components



a)



b)



c)

Figure 13. Variations of seismic noise during a day for the period of 10-30s.
a) Z components, b) N components, c) E components

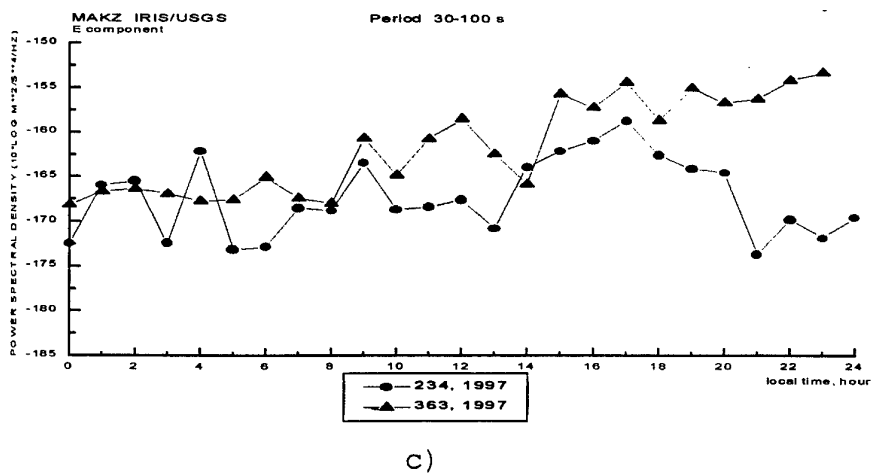
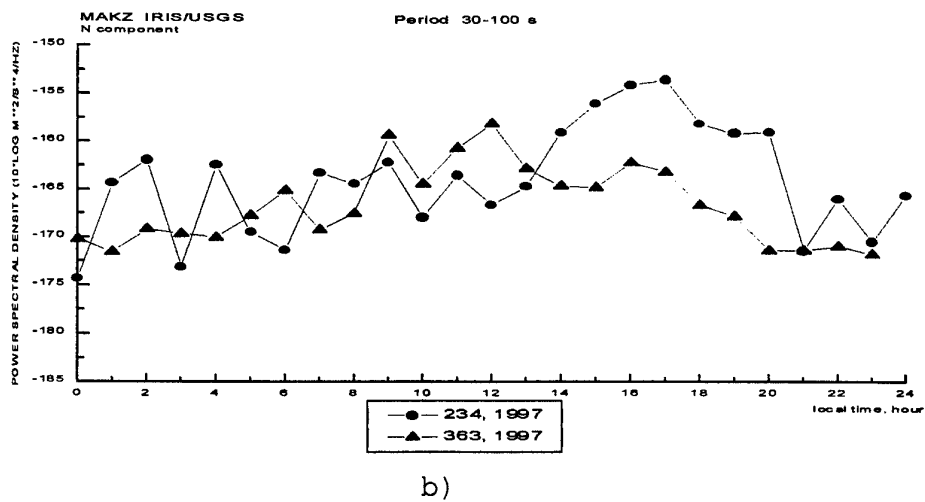
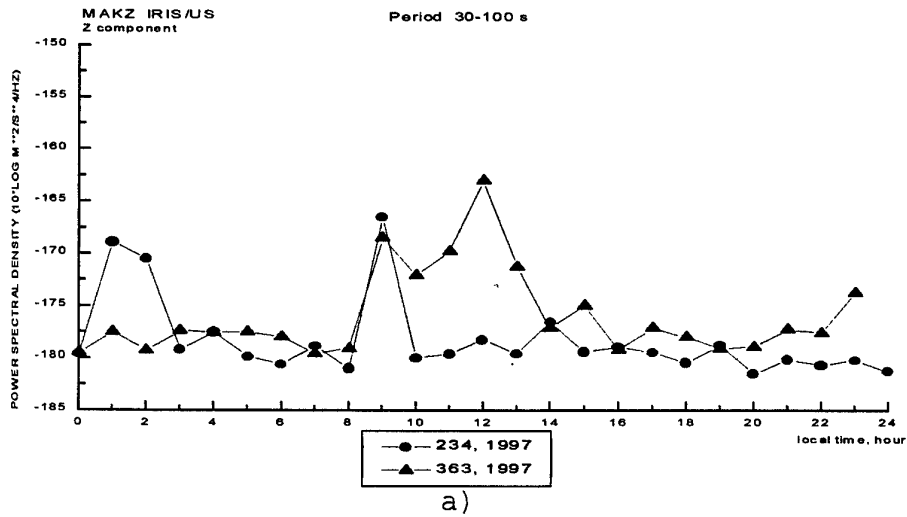
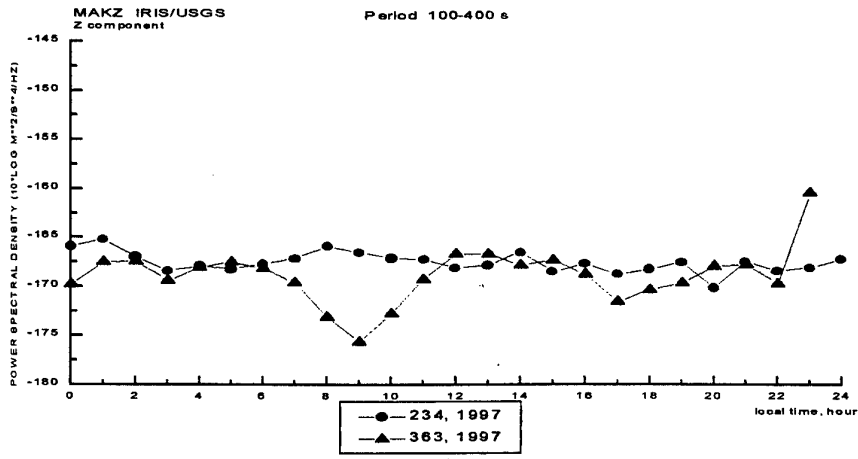
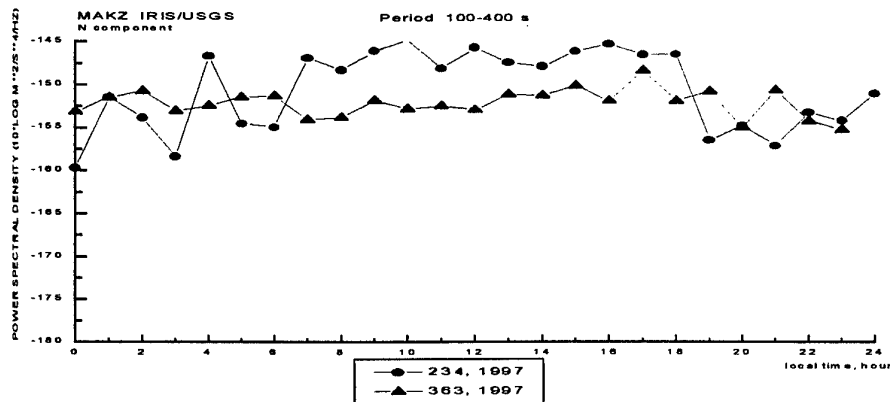


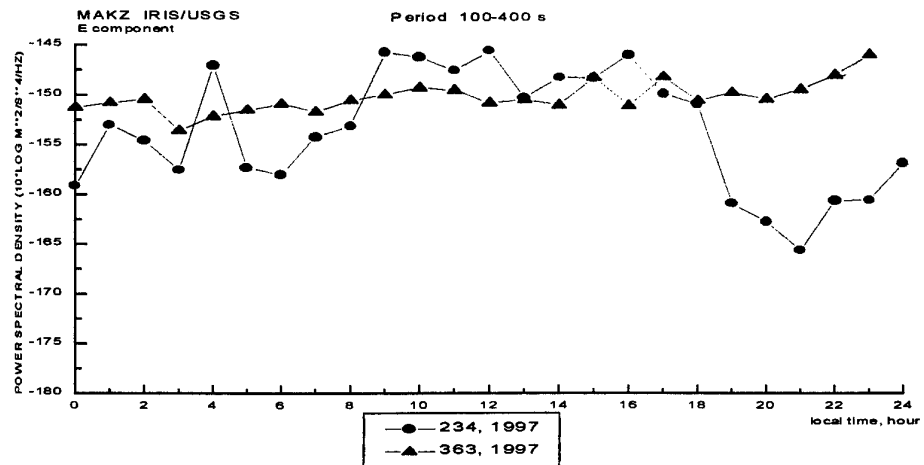
Figure 14 Variations of seismic noise during a day for the period of 30-100s.
a) Z components, b) N components, c) E components



a)



b)



c)

Figure 15. Variations of seismic noise during a day for the period of 100-400s.
a) Z components, b) N components, c) E components

(Figure 15) daily variations on horizontal components (from 7-8 to 18 hours local time) appears. It is caused by long-period oscillations on horizontal components (see Figure 5).

So, the following conclusion can be made. First, the seismic noise on Makanchi station is influenced by industrial activity, that is seen from daily variations of noise level, especially on high frequencies, which is higher during a day, and lower during a night. Second, the seasonal variations of noise level are present. They are manifested by different pattern of daily variations for winter and summer days, and by dependence of noise level from season of the year. This dependence is different for different periods: for high frequencies the noise level on winter is lower than in summer, for periods 1-10 sec, on a contrary, the noise level on winter is higher than in summer.

Seasonal variations. Figure 16-18 show noise spectra computed for all four seasons of the year, separately for days and nights.

The median and extreme values of noise. The study of the distribution of variations of noise spectra during the all time of observations caused by influence of natural as well as industrial factors have been made. The analysis was made for day and for night noise spectra separately.

The empirical distribution was described by two parameters not depended of the distribution curve: the median $MeS(T)$, where $S(T)$ - is a noise spectra, and extreme values: lowest (10% percentile) - $[MeS(T) - \sigma^-(T)]$, and highest (90% percentile) - $[MeS(T) + \sigma^+(T)]$, where $\sigma^-(T)$ and $\sigma^+(T)$ are biases from median. The median spectra as well as percentile spectra for all components for day and night are shown on Figure 19,20,21.

The values of $\sigma^-(T)$ and $\sigma^+(T)$, significantly depend on the frequency band. They are minimal for the periods, where seismic noise on Makanchi station is closest to the low noise model - from 2,5 to 10 sec. The $[MeS(T) - \sigma^-(T)]$ curve for Makanchi station for this period almost coincides with low noise model. Outside this period, the variations of $\sigma^-(T)$ and $\sigma^+(T)$ increase. The values of $\sigma^-(T)$ and $\sigma^+(T)$ vary from $\sigma^+, \sigma^- = 2,5$ dB up to $\sigma^+_{max} = 12$ dB, and $\sigma^-_{max} = 7$ dB. So, the natural variations of noise level in all cases (for all components, for all periods) are less then 10% from $MeS(T)$.

6. The records of underground nuclear explosions and earthquakes.

The last underground nuclear explosion on the Lobnor test site was made on the July 29, 1996. At that time the seismic station PASSCAL was operated on Makanchi observatory. Data on PASSCAL station were recorded in Reftek format. Unfortunately, at present time, there is no way to make a correct analysis of spectra of nuclear explosions and earthquakes, because, by methodical

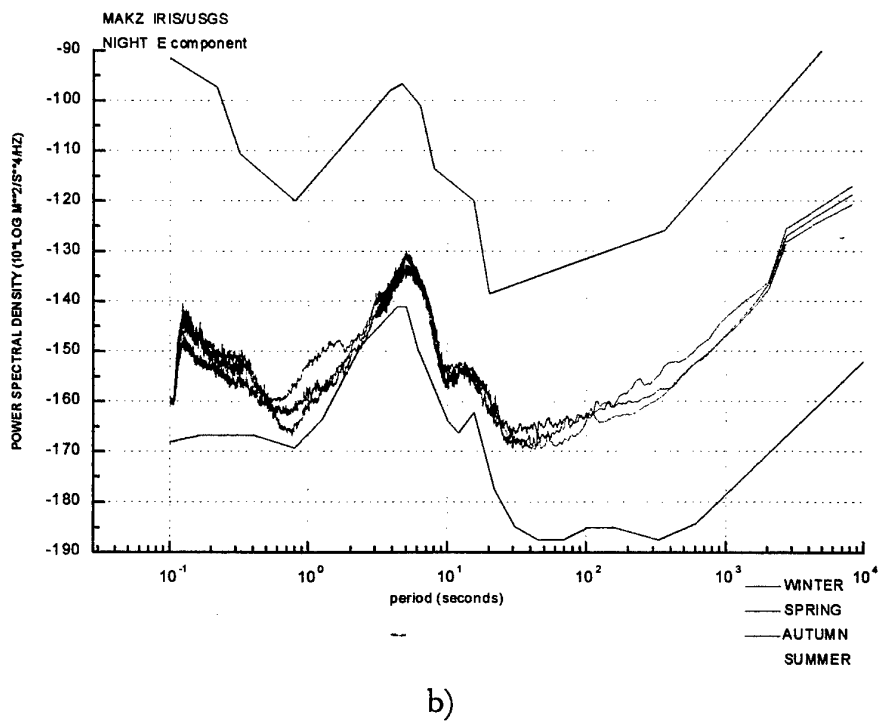
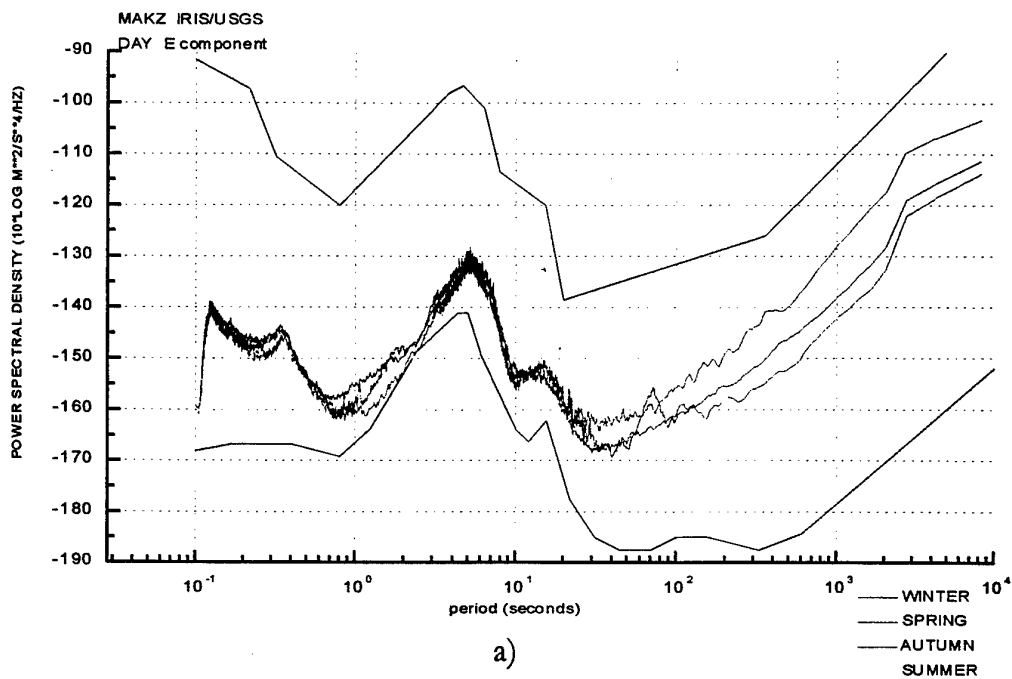
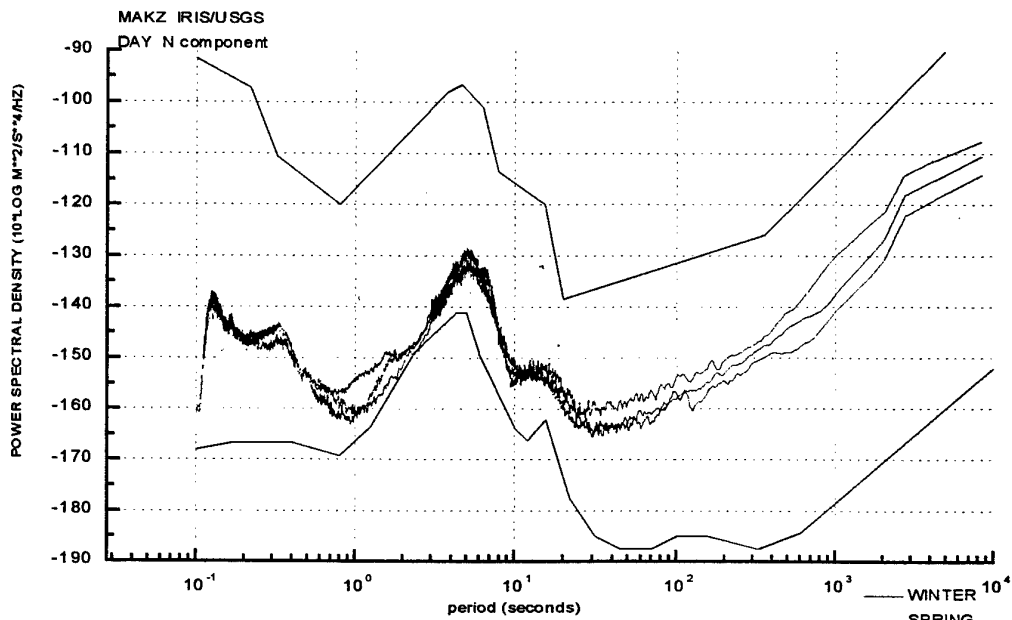
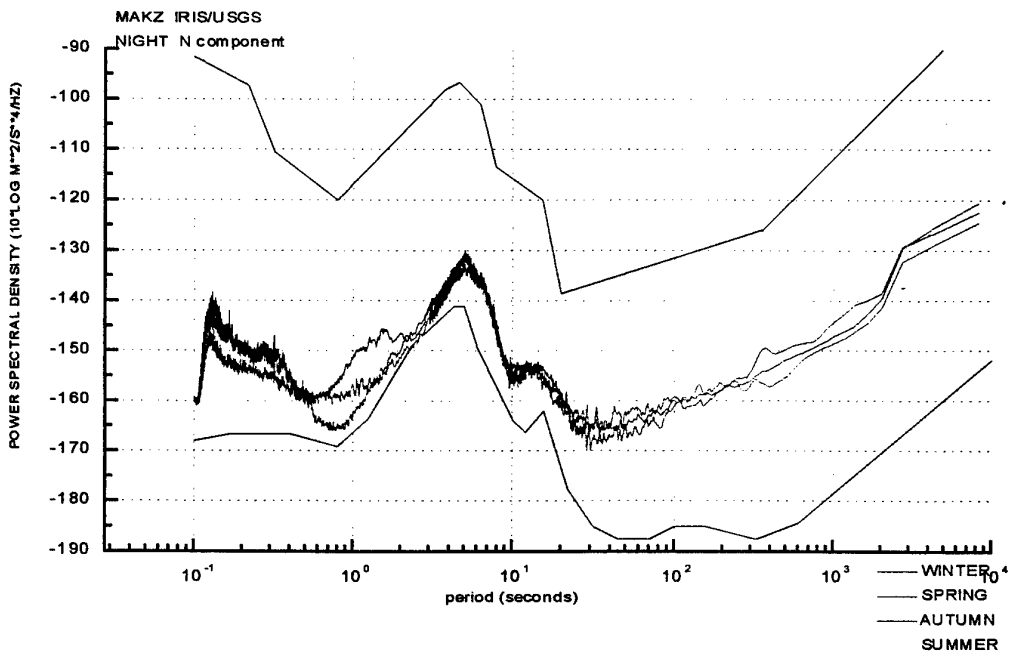


Figure 16. Seasonal variations of seismic noise for E component : a) day; b) night.

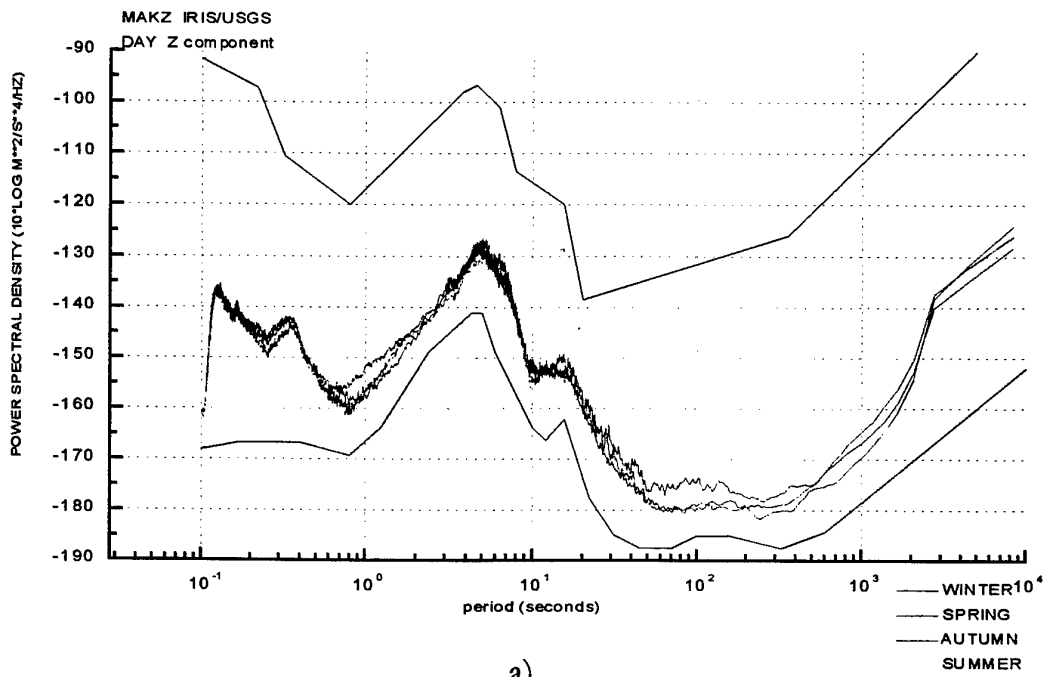


a)

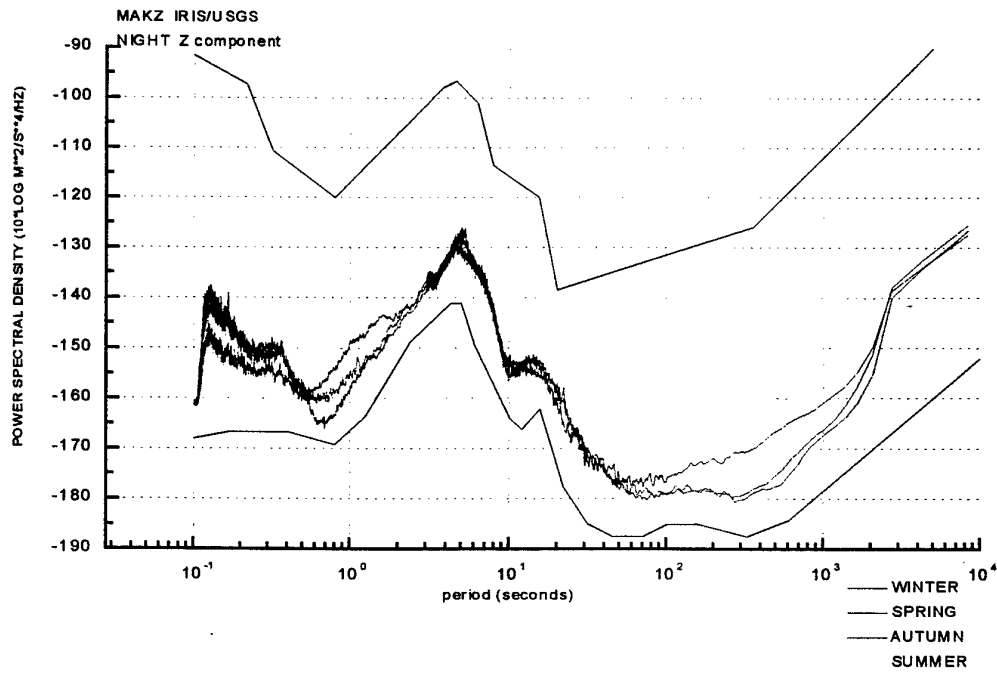


b)

Figure 17. Seasonal variations of seismic noise for N component : a) day, b) night.

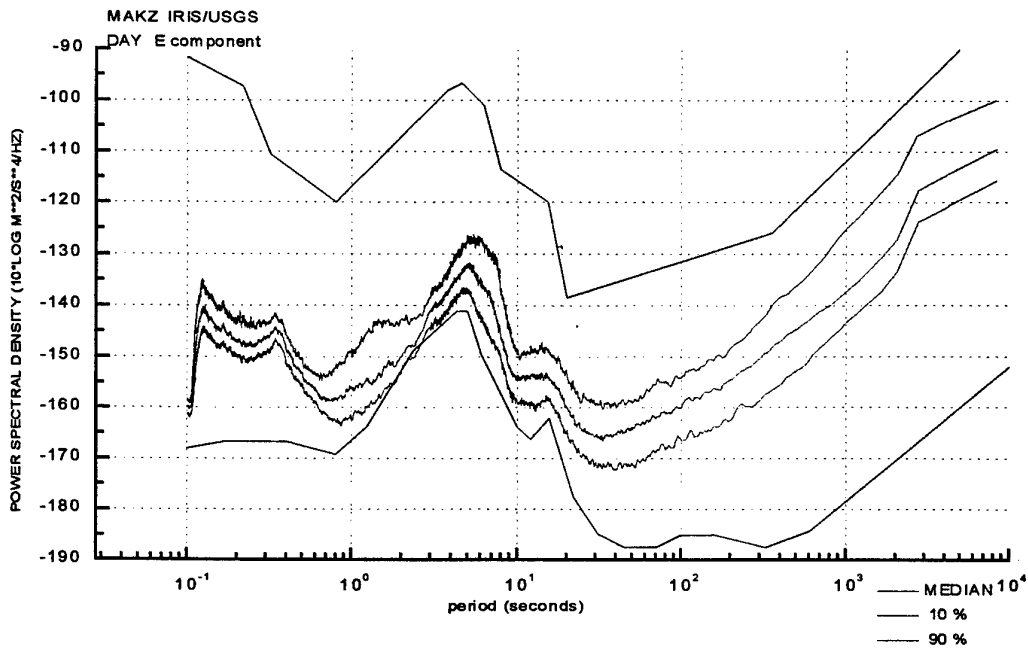


a)

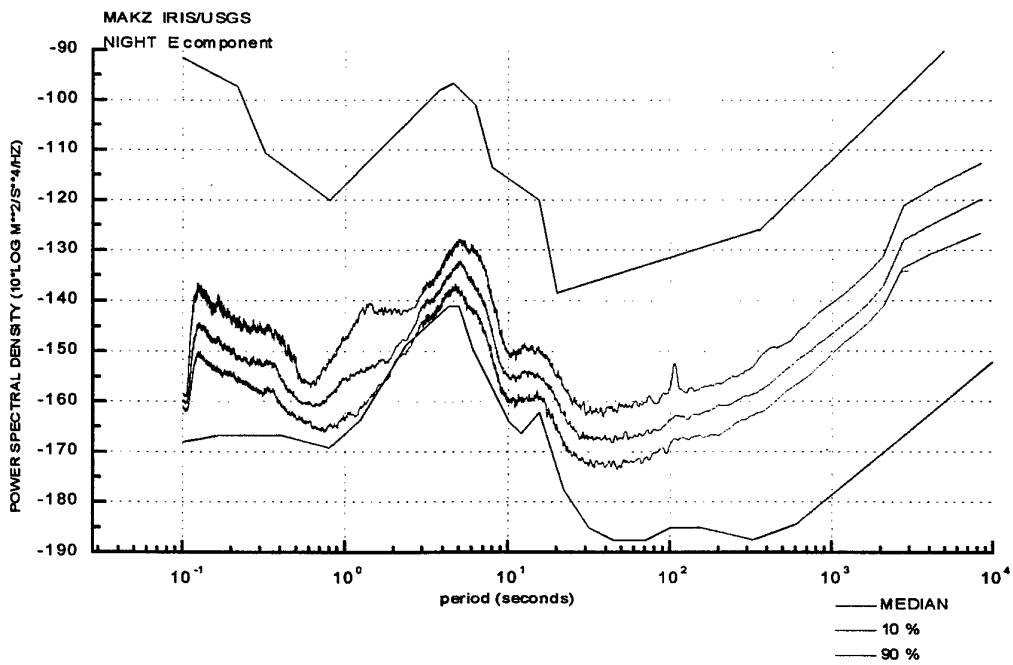


b)

Figure 18. Seasonal variations of seismic noise for Z component : a) day, b) night.



a)



b)

Figure 19. Median (50%) and extreme (90% and 10%) spectra values for E component: a) day, b) night.

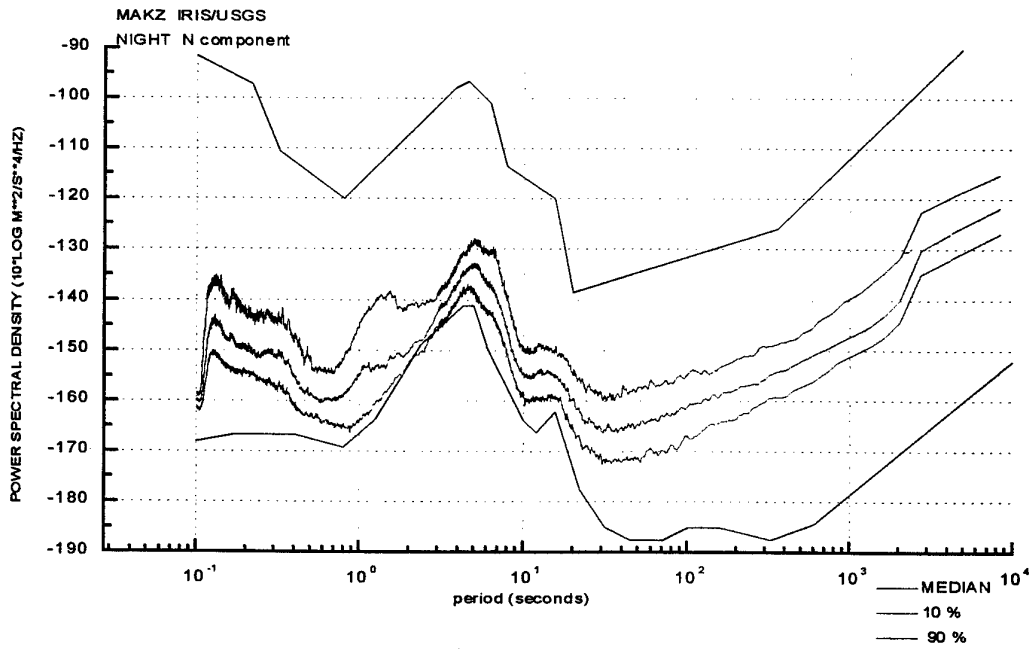
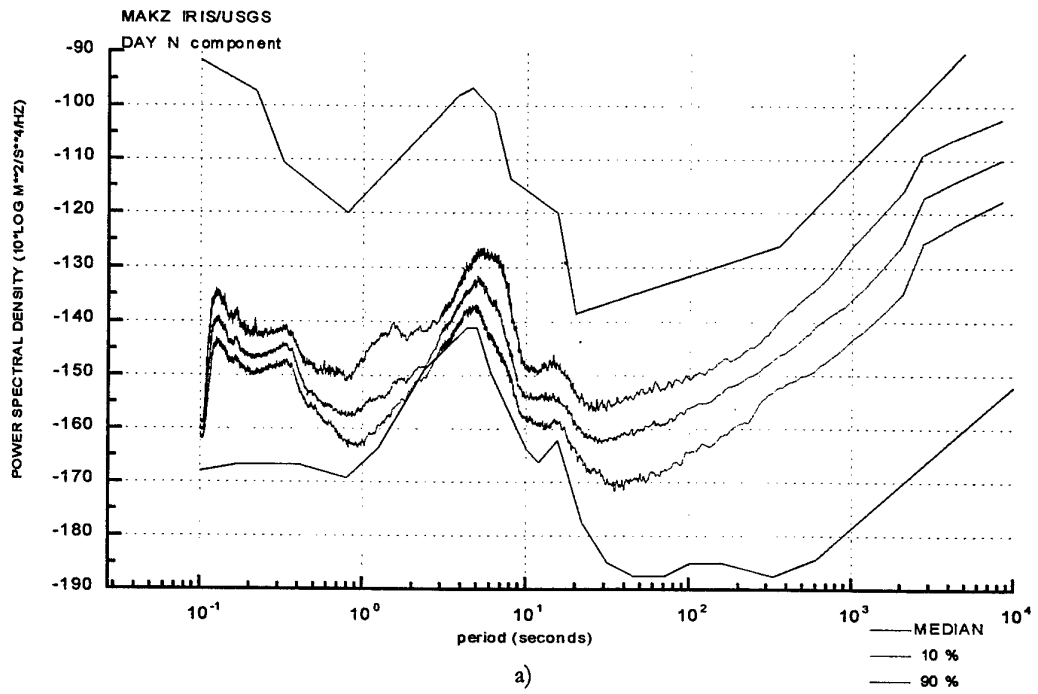
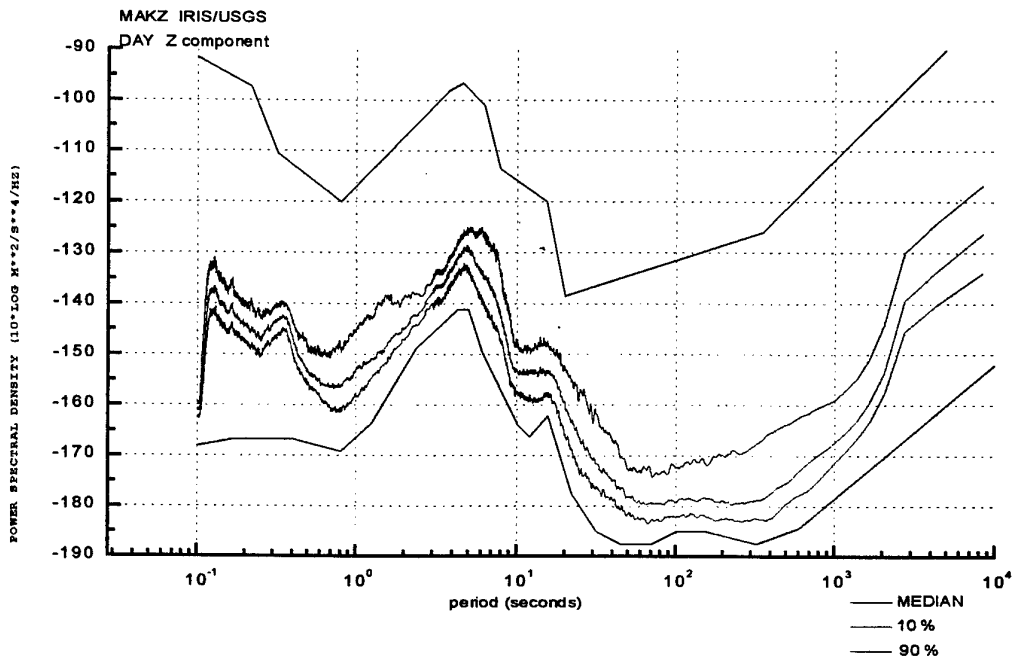
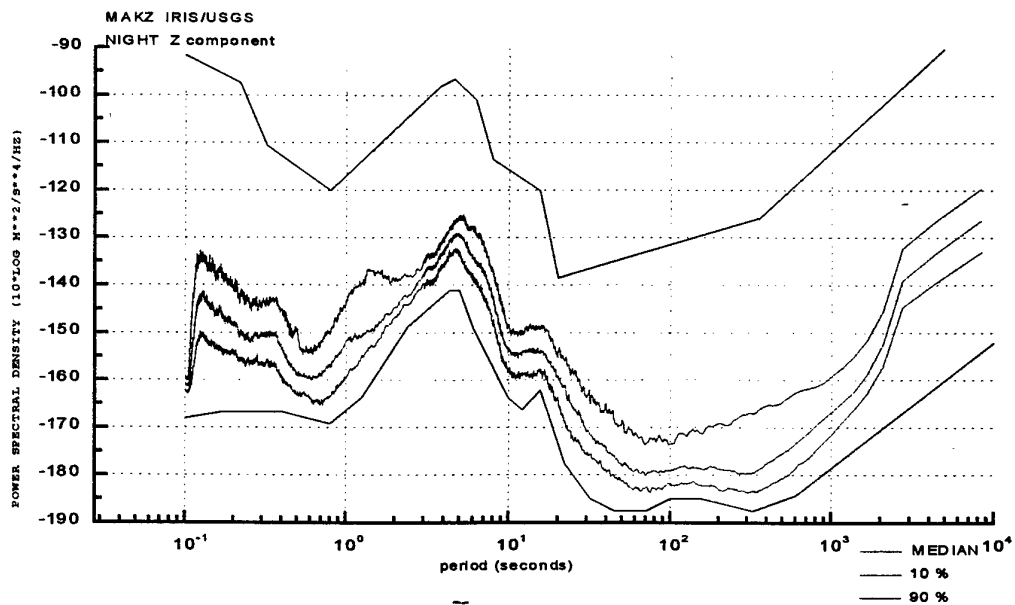


Figure 20. Median (50%) and extreme (90% and 10%) spectra values for N component: a) day, b) night.



a)



b)

Figure 21. Median (50%) and extreme (90% and 10%) spectra values for Z component: a) day, b) night.

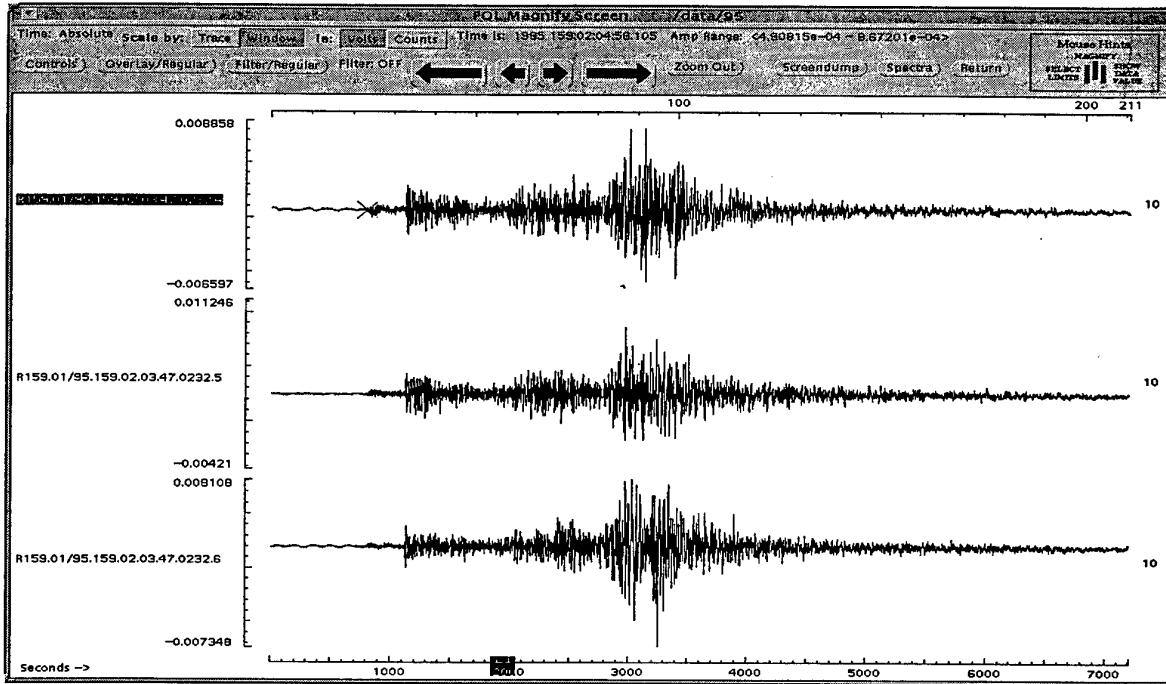


Figure 22. An example of earthquake near Lobnor test site. 8/6/1995, Lat=43,016N, Lon=83,259E, D=433 km, Ms=4,3, length of record is about 3,5 min.

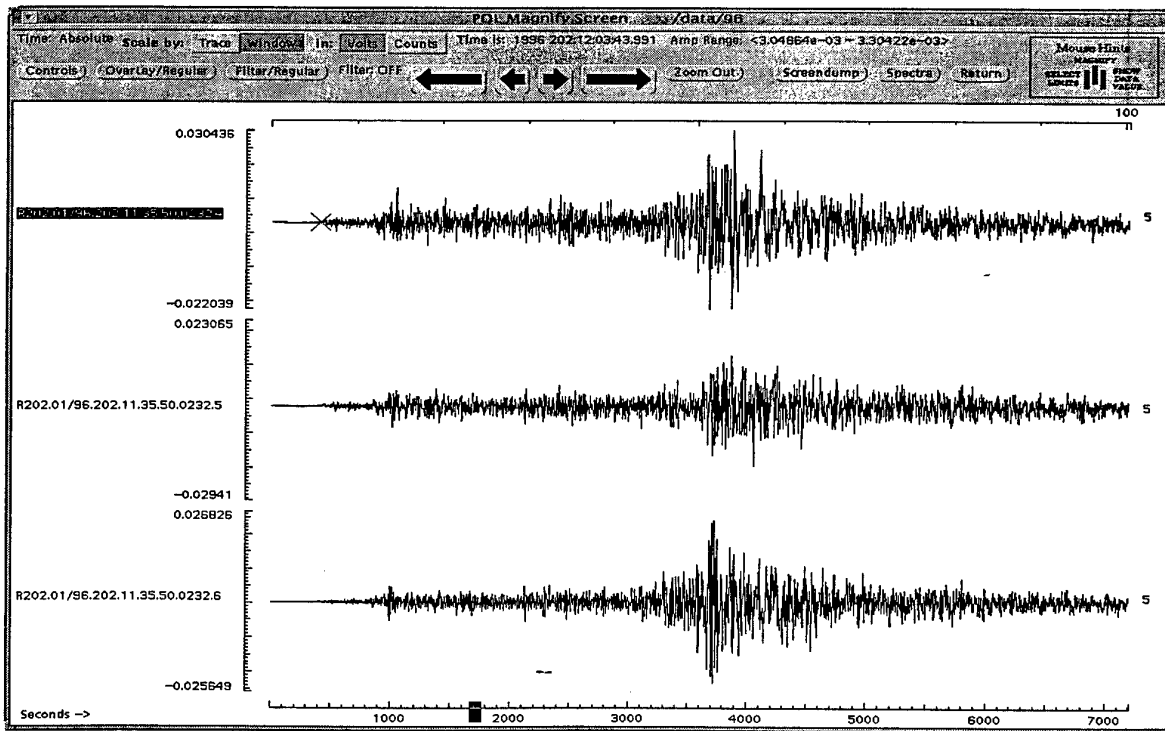


Figure 23. An example of earthquake near Lobnor test site. 20/7/1996, Lat= 43,983N, Lon= 3,596E, Ms=4,5, D=338 km. Length of record is about 100 sec.

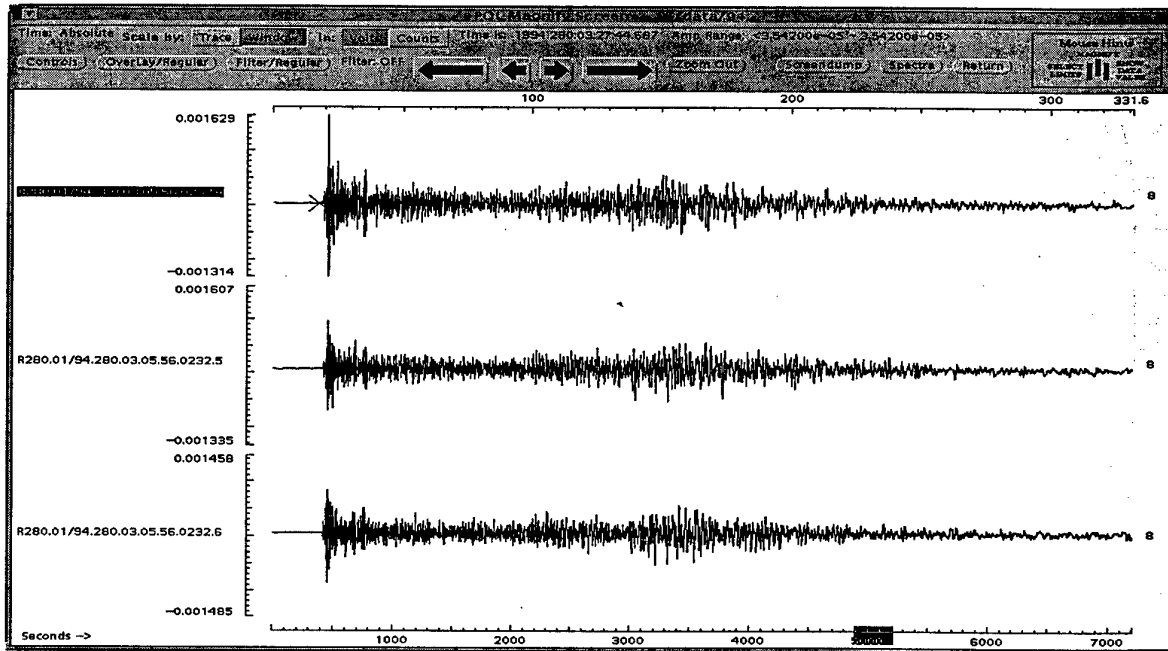


Figure 24. Underground nuclear explosion on Lobnor test site. 7/10/1994.
 Lat=41,662N, Lon=88,753E. D=786 km. Ms=6,0, length of record is about 5,5 min.

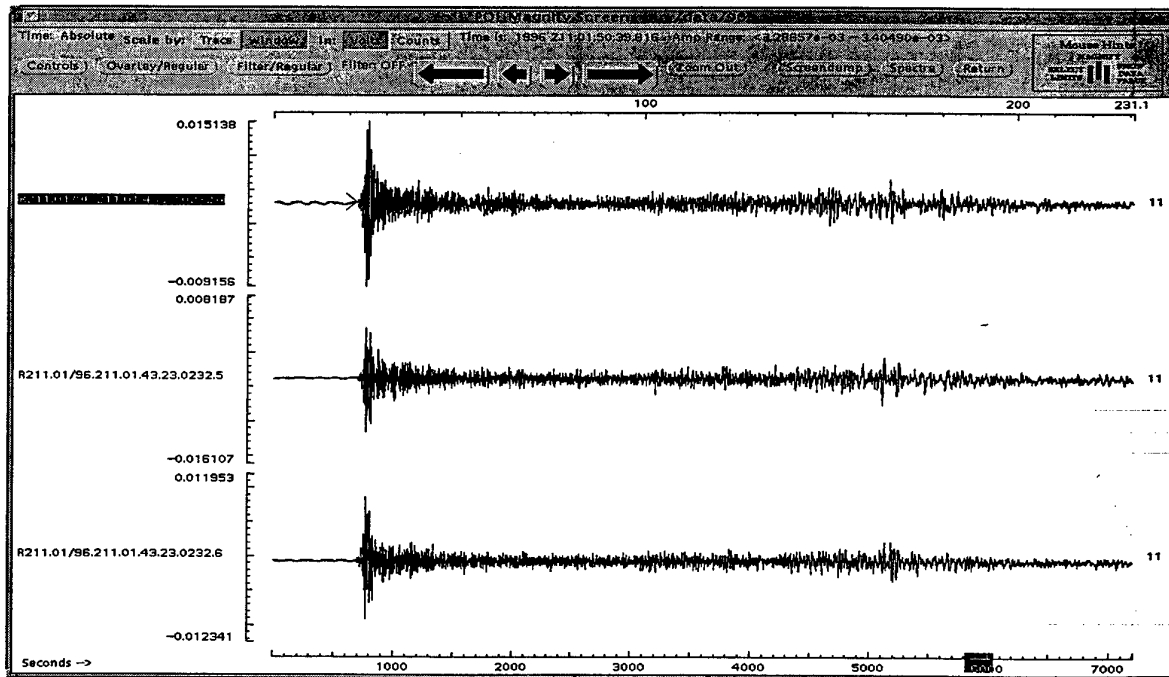


Figure 25. Underground nuclear explosion on Lobnor test site. 29/7/1996,
 Lat=41,824N, Lon=88,420E, D=754 km, Ms=4,9, length of record is about 4 min.

obstacles, there were no possibility to make correction for instrument response of PASSCAL station, installed at that time.

The records of two nuclear explosions, conducted at Lobnor test site, and two earthquakes, occurred in the nearby area, are shown on Figure 22-25.

Conclusion

1. The noise spectra for Makanchi station have been studied in a whole range of frequencies. For the period 0,5 -20 sec noise spectra is close to the low noise model. This result allows to consider the Makanchi station as a sensitive station of GSN. The seismic spectra earthquakes and underground nuclear explosions, recorded on regional distances, fall exactly on this period.

2. In the long-period band, Makanchi station is rather noisy. The unknown source, most probable of artificial origin, does exist, which generates long-period noise, polarized in horizontal plane during day time.

3. The variations of noise level on various frequencies were studied. The noise level near the station is affected as by industrial as well as by natural sources of microseism. Quantitatively, variations of seismic noise level, caused by industrial sources and natural sources are of the same order - less than 10% from the median noise level. However, the industrial noise has clearly marked periods, whereas natural variations occur in the all periods of noise spectra.

Authors express deep gratitude to doctor W.-Y. Kim from Lamont Doherty Earth Observatory of Columbia University (USA), for the program POWER afforded by him, as well as for the help and consultation rendered by him during the execution of present work.

References.

1. Геологическая карта Лист -44-X, объяснительная записка, масштаб 1:200000, издание 1961 год, Гольшев С.Н., Твердислов Ю.А. и другие.

2. Геологическая карта Лист -44-XI, объяснительная записка, масштаб 1:200000, издание 1963 год, Преображенская О.Т. и другие.

3. William H. Press, Brian P. Flannery, Saul A. Teukolsky, William T. Vetterling. Numerical Recipes. Cambridge University Press, 1987 year, 818 pp.

4. Jon Peterson, Observation and Modeling of Seismic Background Noise. Open-File Report 93-322, Albuquerque, New Mexico, 1993 year, 42 pp.